G-2 Internal
Version 1.0
August 13, 2019

# On the background correction of the Cornell fast rotation Fourier analysis

J. Fagin[1], A. Chapelain[1], D. Rubin[1], and D. Seleznev[1]
[1]Cornell University

**Abstract**

The muon frequency distribution is found by taking the cosine Fourier transformation of the fast rotation signal. The cosine Fourier transformation should begin at a time $t_0$ when the centroid of the time profile of the muon beam first passes the detector. We want to start the Fourier transform at a later start time $t_s$ in order to skip the beam-line positron contamination of the muon beam which continues for the first 4 $\mu$s and possibly to skip scraping which lasts for the first 30 $\mu$s of the fast rotation signal. The missing time between $t_0$ and $t_s$ of the cosine Fourier transformation must be accounted for. This missing time creates a background on the cosine Fourier transformation which must be removed. We fitted the background and then subtract it to recovered the complete frequency distribution.

The background can be fitted using different functions which are all equivalent for values of $t_s$ of at least 4 $\mu$s, enough to skip the positron contamination. The background can be fitted accurately for values of $t_s$ up to 25 $\mu$s for both Gaussian and asymmetric Monte Carlo fast rotation signals using some fit functions. For frequency distributions with higher statistics and less width, we would likely be able to fit the background all the way up to 30 $\mu$s allowing us to skip all of scraping.

We also offer an alternative approach by first approximate the frequency distribution and then using the approximation to calculate the background. An iterative process can be used which self corrects the background allowing us to instead start with the cosine Fourier transformation as the approximate frequency distribution. These approaches work precisely for values of $t_s$ of at least 4 $\mu$s but falter when $t_s$ is greater than 8 $\mu$s.

## Contents

# 1 Introduction

The goal of the fast rotation Fourier analysis is to calculate the E-field correction to $\omega_a$ which is the precession frequency of the muon's spin about its momentum. The E-field correction is directly calculated from the radial distribution of the muons which is produced from the frequency distribution. To calculate the E-field correction, we must be able to extract the frequency distribution from the fast rotation signal to a high degree of accuracy [1].

The frequency distribution of the muons about the ring is obtained by doing a Fourier transformation of the fast rotation signal. The fast rotation signal is the change in the intensity of the muons as they go around the ring at a fixed location. since the frequency distribution of the muons is approximately even about its center, the frequency distribution is obtained by taking the real part of the Fourier transformation, which is the cosine Fourier transformation [2].

When taking the cosine Fourier transformation of the fast rotation signal, we must skip the first several microseconds of data because there is beam-line positron contamination of the muon beam which is gone by 4 $\mu$s . Figure 1 shows the beam-line positron contamination of the muon beam on the first first 4 $\mu$s of the fast rotation signal for the Run-1 60-hour data set. The first 30 $\mu$s of the fast rotation signal is afflicted by scraping which may affect the radial distribution of the muons, so ideally we also want the ability skip this as well.

The cosine Fourier transformation ideally begins at the time when the centroid of the time profile of the muon beam first passes the detector denoted as $t_0$. We must instead start the cosine Fourier transformation of the fast rotation signal not at $t_0$ but instead a later start time $t_s$ to skip the positron contamination and ideally scraping. To recover an accurate frequency distribution, the missing time in the cosine Fourier transform between $t_0$ and $t_s$ must be accounted for.

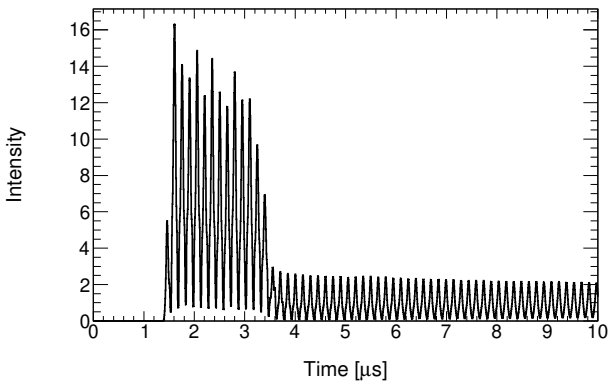


Figure 1: The first 10 $\mu$s of the fast rotation signal is shown for Run-1 60-hour data set. The positron interference can be seen in the first 4 $\mu$s of the signal.

For a fast rotation signal S(t), the frequency distribution $\tilde{S}(\omega)$ can be recovered via the cosine Fourier transform [2]:

$$\tilde{S}(\omega) \;=\; \sqrt{\frac{2}{\pi}}\int_{t_0}^{\infty} S(t)\cos\omega(t\,-\,t_0)dt \;=\; \sqrt{\frac{2}{\pi}}\int_{t_s}^{\infty} S(t)\cos\omega(t\,-\,t_0)dt + \sqrt{\frac{2}{\pi}}\int_{t_0}^{t_s} S(t)\cos\omega(t\,-\,t_0)dt. \quad (1)$$

The integral between $t_0$ and $t_s$ is the correction to the fast rotation signal denoted $\Delta(\omega)$. The correction is equal to the following equation where $\omega^+ = 6.748$ MHz and $\omega^- = 6.663$ MHz are the bounds of the collimator aperture [2]:

$$\Delta(\omega) = \sqrt{\frac{2}{\pi}}\int_{t_0}^{t_s} S(t)\cos\omega(t-t_0)dt \approx \frac{1}{\pi}\int_{\omega^-}^{\omega^+} \tilde{S}(\omega\prime)\frac{\sin[(\omega-\omega\prime)(t_s-t_0)]}{\omega-\omega\prime}d\omega\prime. \quad (2)$$

We add the correction to the cosine Fourier transformation in order to recover the complete frequency distribution. We do this by fitting for the background to the cosine Fourier transformation which is the negative of the correction. Then we subtract the background from the cosine Fourier transformation yielding the complete frequency distribution.

**Important note**: The equation (2) above and all the other equations in this note use angular frequencies $\omega$, however all figures are shown using frequency $f$ where $\omega = 2\pi f$. Using angular frequency makes calculations

clearer, but to get physically meaningful figures all angular frequencies must be converted to regular frequencies by dividing by $2\pi$.

## 2 Analytic forms of the background of the cosine Fourier transform

The goal of this work is to derive general analytical forms of the cosine Fourier transform background in order to be able to fit for it and therefore correct for it for simulated and real data. Analytical frequency distributions with increasing complexity and realism will be plugged into equation (2). The analytical form of the cosine Fourier transform in the real data is not known but a general enough background form will be a good approximation.

### 2.1 Dirac delta frequency distribution

For an arbitrary frequency distribution $\tilde{S}(\omega)$ confined within the collimator aperture at $\omega^-$ and $\omega^+$, we know the form of the correction to the cosine Fourier transformation of the fast rotation signal is given by the following equation:

$$\Delta(\omega) = \frac{1}{\pi}\int_{\omega^-}^{\omega^+} \tilde{S}(\omega\prime)\frac{\sin[(\omega-\omega\prime)(t_s-t_0)]}{\omega-\omega\prime}d\omega\prime. \tag{3}$$

We will first assume that the frequency distribution is a Dirac delta function centered at a frequency $\omega_0$:

$$\tilde{S}(\omega) = \delta(\omega-\omega_0). \tag{4}$$

We start with a Dirac delta function because it is the simplest function to integrate and only has a single defining parameter which is its center. We plug the delta function ansatz into equation (3):

$$\Delta(\omega) = \frac{1}{\pi}\int_{\omega^-}^{\omega^+} \delta(\omega\prime-\omega_0)\frac{\sin[(\omega-\omega\prime)(t_s-t_0)]}{\omega-\omega\prime}d\omega\prime = \frac{1}{\pi}\frac{\sin[(\omega-\omega_0)(t_s-t_0)]}{(\omega-\omega_0)}. \tag{5}$$

The background in equation (6) takes the form of a sinc function since:

$$\Delta(\omega) = \frac{(t_s-t_0)}{\pi}\,\mathrm{sinc}[(\omega-\omega_0)(t_s-t_0)]. \tag{6}$$

We show in figure 2 the background for a Dirac delta function centered at the magic frequency with different start times. The magic frequency is at 6.705 MHz. The input frequency distribution is the same Dirac delta function each time, but the background changes with $t_s$.

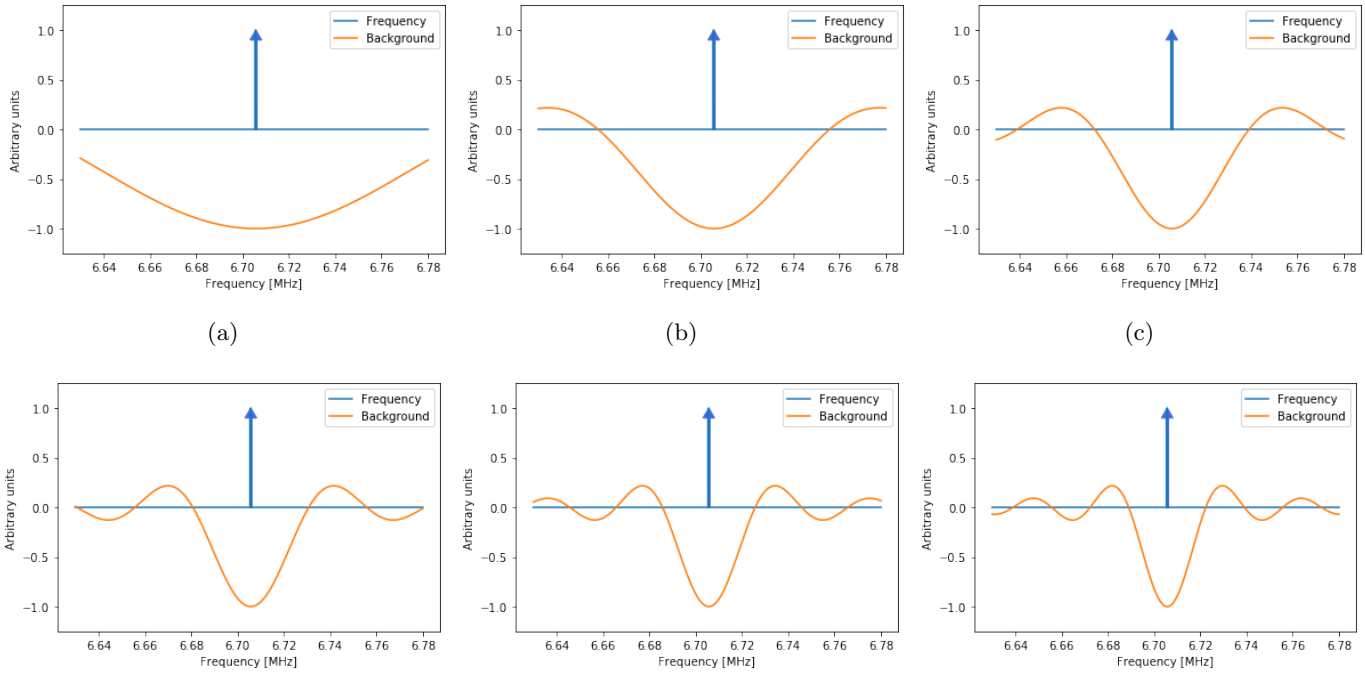


Figure 2: Background with $t_0 = 0$ $\mu$s and different values of $t_s$ for a Dirac delta function frequency distribution centered at the magic frequency. Six start times are shown: (a) 5 $\mu$s, (b) 10 $\mu$s, (c) 15 $\mu$s, (d) 20 $\mu$s, (e) 25 $\mu$s, (f) 30 $\mu$s.

### 2.2 Step function frequency distribution

The work done in the previous section assumed a Dirac delta frequency distribution. We can make a similar derivation using a step function frequency distribution. We choose to use a step function because we are still able to integrate it into equation (3) and it is a more realistic frequency distribution than a delta function since the muon beam must have some spread around the ring.

The step function frequency distribution is defined between $\omega_1$ and $\omega_2$ where $\omega_1$ and $\omega_2$ are within the bound of the collimator aperture and $\omega_2 > \omega_1$. Then we have a normalized frequency distribution as follows:

$$\tilde{S}(\omega) = \frac{1}{\omega_2 - \omega_1} \begin{cases} 1 & \omega_1 \leq \omega \leq \omega_2 \\ 0 & \text{else} \end{cases} \tag{7}$$

When we plug this directly into our equation for the background correction (3):

$$\Delta(\omega) = \frac{1}{\pi(\omega_2 - \omega_1)} \int_{\omega_1}^{\omega_2} \frac{\sin[(\omega - \omega\prime)(t_s - t_0)]}{\omega - \omega\prime} d\omega\prime = \frac{1}{\pi(\omega_2 - \omega_1)} \big[ \text{Si}((\omega - \omega_1)(t_s - t_0)) - \text{Si}((\omega - \omega_2)(t_s - t_0)) \big], \tag{8}$$

where the Si function is defined as:

$$\text{Si}(x) = \int_0^x \frac{\sin(y)}{y} dy. \tag{9}$$

Using a step function frequency distribution is a large improvement from the Dirac delta function since we can enclose any frequency distribution within a step function as a rough approximation for the correction to

the cosine Fourier transformation. The Dirac delta function only had a single characteristic parameter which was its center. The step function frequency distribution has two characteristic parameters corresponding to each bound of the step function. This additional parameter is an extra degree of freedom when fitting the background which makes the fit work for much larger values of $t_s$. Figure 3 shows the background for a step function centered at the magic frequency with a width of 10 kHz.

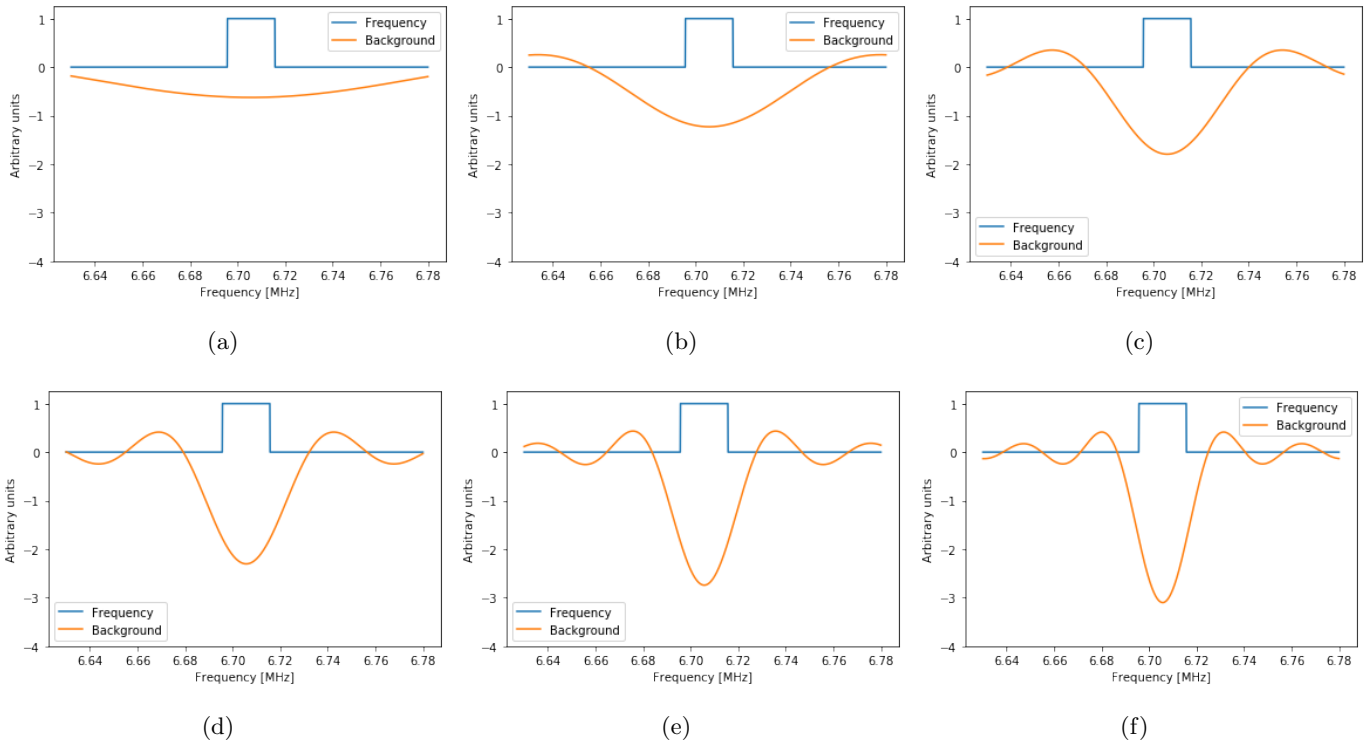


Figure 3: Background with $t_0 = 0$ $\mu$s and different values of $t_s$ for a step function frequency distribution centered at the magic frequency and a width of $\pm 10$ kHz. Six start times are shown: (a) 5 $\mu$s, (b) 10 $\mu$s, (c) 15 $\mu$s, (d) 20 $\mu$s, (e) 25 $\mu$s, (f) 30 $\mu$s.

### 2.3 Gaussian frequency distribution

We now consider a Gaussian frequency distribution since it is more realistic than the step function because the muon beam for real data is smooth without the jagged corners that a step function has. We assume a Gaussian frequency distribution centered at the magic frequency $\omega_0$ with standard deviation $\sigma$:

$$\tilde{S}(\omega) = \frac{1}{\sqrt{2\pi\sigma^2}} e^{-\frac{(\omega-\omega_0)^2}{2\sigma^2}}. \tag{10}$$

We then plug the Gaussian frequency distribution directly into equation (3):

$$\Delta(\omega) = \frac{1}{\pi} \int_{\omega^-}^{\omega^+} \frac{1}{\sqrt{2\pi\sigma^2}} e^{-\frac{(\omega\prime-\omega_0)^2}{2\sigma^2}} \frac{\sin[(\omega-\omega\prime)(t_s-t_0)]}{\omega-\omega\prime} d\omega\prime. \tag{11}$$

Physical frequency distributions must be confined within the collimator aperture since the muon beam must exist within the ring. We assume a Gaussian frequency distribution who's full 5-standard-deviation width is contained within the collimator aperture. Therefore, we evaluate the integral with arbitrarily large bounds

since the Gaussian will be close to zero outside the physical frequency range. This is necessary so that the integral can be evaluated analytically.

$$\Delta(\omega) = \frac{1}{\sqrt{2\pi^3\sigma^2}} \int_{-\infty}^{+\infty} e^{-\frac{(\omega\prime-\omega_0)^2}{2\sigma^2}} \frac{\sin[(\omega-\omega\prime)(t_s-t_0)]}{\omega-\omega\prime} d\omega\prime, \tag{12}$$

and now we can evaluate the integral:

$$\begin{aligned}
\Delta(\omega) &= \frac{1}{\sqrt{2\pi^3\sigma^2}} \int_0^{t_s-t_0} dt \int_{-\infty}^{+\infty} e^{-\frac{(\omega\prime-\omega_0)^2}{2\sigma^2}} \cos(\omega-\omega\prime)t d\omega\prime \\
&= \frac{1}{\sqrt{2\pi^3\sigma^2}} \int_0^{t_s-t_0} dt \,\mathrm{Re}\Big\{ \int_{-\infty}^{+\infty} e^{-\frac{(\omega\prime-\omega_0)^2}{2\sigma^2}+i(\omega-\omega\prime)t} d\omega\prime \Big\} \\
&= \frac{1}{\sqrt{2\pi^3\sigma^2}} \int_0^{t_s-t_0} dt \,\mathrm{Re}\Big\{ \int_{-\infty}^{+\infty} e^{-\frac{\omega\prime^2}{2\sigma^2}+(\frac{\omega_0}{\sigma^2}-it)\omega\prime+i\omega t-\frac{\omega_0^2}{2\sigma^2}} d\omega\prime \Big\}.
\end{aligned} \tag{13}$$

The inner integral can be evaluated since it is a standard Gaussian integral of a degree two polynomial. It is solved by completing the square as follows:

$$\begin{aligned}
\Delta(\omega) &= \frac{1}{\sqrt{2\pi^3\sigma^2}} \int_0^{t_s-t_0} dt \,\mathrm{Re}\Big\{ \sqrt{2\pi\sigma^2} e^{\frac{\sigma^2}{2}(\frac{\omega_0}{\sigma^2}-it)^2+i\omega t-\frac{\omega_0^2}{2\sigma^2}} \Big\} = \frac{1}{\pi} e^{\frac{-\omega_0^2}{2\sigma^2}} \,\mathrm{Re}\Big\{ \int_0^{t_s-t_0} e^{\frac{\sigma^2}{2}(\frac{\omega_0}{\sigma^2}-it)^2+i\omega t} dt \Big\} \\
&= \frac{1}{\pi} e^{\frac{-\omega_0^2}{2\sigma^2}} \,\mathrm{Re}\Big\{ i\sqrt{\frac{\pi}{2\sigma^2}} e^{-\frac{\omega_0\omega}{\sigma^2}-\frac{\omega^2}{2\sigma}} \Big[ \mathrm{erfi}\,(\frac{\omega-\omega_0}{\sqrt{2\sigma^2}}) - \mathrm{erfi}\,(\frac{\omega-\omega_0+i\sigma^2(t_s-t_0)}{\sqrt{2\sigma^2}}) \Big] \Big\} \\
&= \frac{1}{\sqrt{2\pi\sigma^2}} e^{\frac{-(\omega-\omega_0)^2}{2\sigma^2}} \,\mathrm{Re}\Big\{ i\Big[ \mathrm{erfi}\,(\frac{\omega-\omega_0}{\sqrt{2\sigma^2}}) - \mathrm{erfi}\,(\frac{\omega-\omega_0+i\sigma^2(t_s-t_0)}{\sqrt{2\sigma^2}}) \Big] \Big\},
\end{aligned} \tag{14}$$

where the error function, erf(x), is defined by the following equation:

$$\mathrm{erf}(x) = \frac{2}{\sqrt{\pi}} \int_0^x e^{-y^2} dy. \tag{15}$$

The imaginary error function is defined such that: $\mathrm{erfi}(x) = -i\,\mathrm{erf}(ix)$. The first erfi function in equation (14) can be eliminated because $i\,\mathrm{erfi}\,(\frac{\omega-\omega_0}{\sqrt{2\sigma^2}})$ will always be imaginary so its real part is zero so:

$$\begin{aligned}
\Delta(\omega) &= \frac{1}{\sqrt{2\pi\sigma^2}} e^{\frac{-(\omega-\omega_0)^2}{2\sigma^2}} \,\mathrm{Re}\Big\{ -i\,\mathrm{erfi}\,(\frac{\omega-\omega_0+i\sigma^2(t_s-t_0)}{\sqrt{2\sigma^2}}) \Big\} \\
&= \frac{1}{\sqrt{2\pi\sigma^2}} e^{\frac{-(\omega-\omega_0)^2}{2\sigma^2}} \,\mathrm{Im}\Big\{ \mathrm{erfi}\,(\frac{\omega-\omega_0+i\sigma^2(t_s-t_0)}{\sqrt{2\sigma^2}}) \Big\}.
\end{aligned} \tag{16}$$

The form of the correction we derived in equation (16) is proportional to the original Gaussian frequency distribution such that:

$$\Delta(\omega) = \tilde{S}(\omega)\,\mathrm{Im}\Big\{ \mathrm{erfi}\,(\frac{\omega-\omega_0+i\sigma^2(t_s-t_0)}{\sqrt{2\sigma^2}}) \Big\}. \tag{17}$$

Similarly to the step function, the Gaussian frequency distribution has two characteristic parameters corresponding to the mean and standard deviation of the Gaussian. The Gaussian and step function therefore have the same number of degrees of freedom, however a Gaussian frequency distribution is a better representative

of real data. Featured in figure 4 is the background calculated using equation (16) with different values of $t_s$ for a frequency distribution centered at the magic frequency with a standard deviation of 5 kHz.

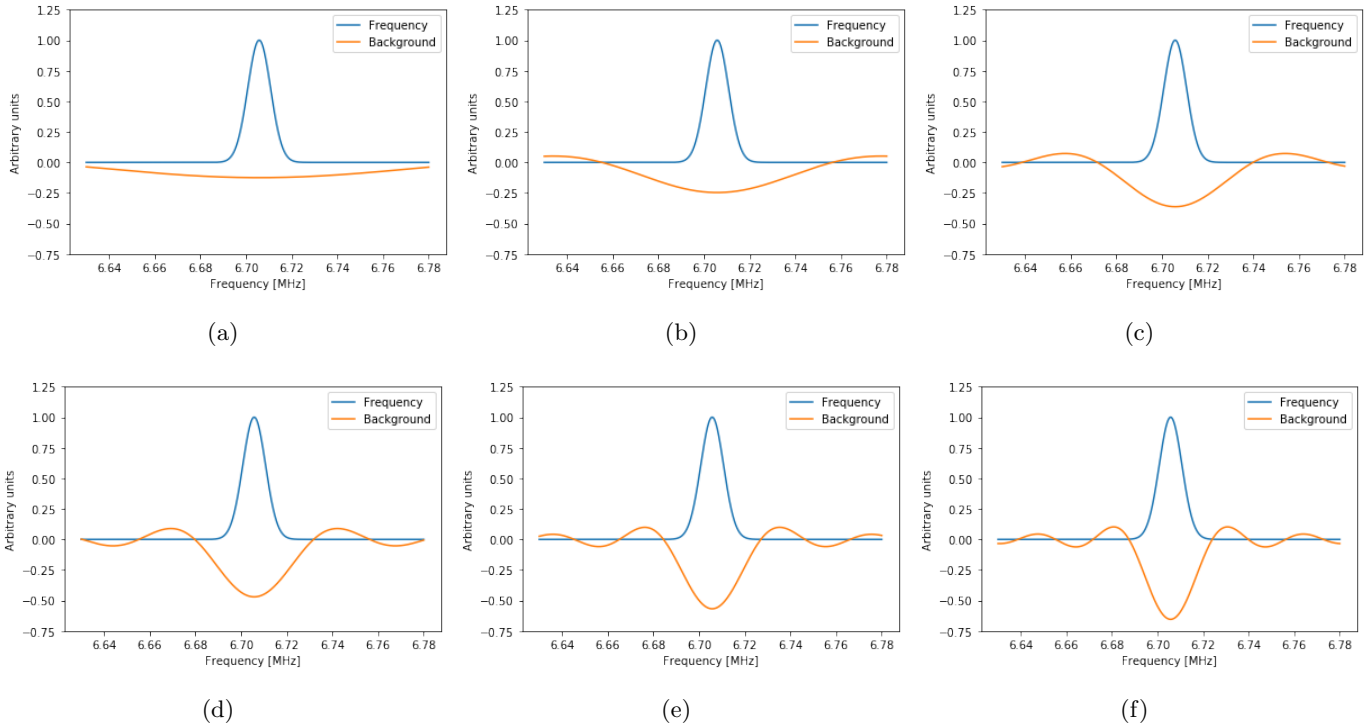


Figure 4: Background with $t_0 = 0$ $\mu$s and different values of $t_s$ for a Gaussian frequency distribution centered at the magic frequency and a standard deviation of 5 kHz. Six start times are shown: (a) 5 $\mu$s, (b) 10 $\mu$s, (c) 15 $\mu$s, (d) 20 $\mu$s, (e) 25 $\mu$s, (f) 30 $\mu$s.

### 2.4 Triangular frequency distribution

We can also derive the form of the correction to the cosine Fourier transform by assuming a triangular frequency distribution. We want to do this because a triangular frequency distribution is very similar to a Gaussian frequency distribution since we can approximately contain a triangle within a Gaussian. The benefit of the triangle is that since it does not have to be symmetric about its center, the analytic form of the correction incorporates asymmetries in the frequency distribution.

We assume the triangle frequency distribution to be zero outside a range of $\omega_1$ and $\omega_2$ where $\omega_1$ and $\omega_2$ are within the bound of the collimator aperture, and the center of the triangle $\omega_0$ is between them such that $\omega_1 \leq \omega_0 \leq \omega_2$. Then we have a normalized triangular frequency distribution of the following form:

$$\tilde{S}(\omega) = \frac{1}{2(\omega_2 - \omega_1)} \begin{cases} \frac{\omega - \omega_1}{\omega_0 - \omega_1} & \omega_1 \leq \omega \leq \omega_0 \\ \frac{\omega_2 - \omega}{\omega_2 - \omega_0} & \omega_0 < \omega \leq \omega_2 \\ 0 & \text{else} \end{cases} \tag{18}$$

We then plug the triangle frequency distribution (18) directly into our equation (3) for the background:

$$\Delta(\omega) = \frac{1}{\pi}\int_{\omega^-}^{\omega^+} \tilde{S}(\omega\prime)\frac{\sin[(\omega-\omega\prime)(t_s-t_0)]}{\omega-\omega\prime}d\omega\prime$$
$$= \frac{1}{2\pi(\omega_2-\omega_1)}\Big[\int_{\omega_1}^{\omega_0}\frac{\omega\prime-\omega_1}{\omega_0-\omega_1}\frac{\sin[(\omega-\omega\prime)(t_s-t_0)]}{\omega-\omega\prime}d\omega\prime + \int_{\omega_0}^{\omega_2}\frac{\omega_2-\omega\prime}{\omega_2-\omega_0}\frac{\sin[(\omega-\omega\prime)(t_s-t_0)]}{\omega-\omega\prime}d\omega\prime\Big]$$
$$= \frac{1}{2\pi(\omega_2-\omega_1)}\Big[\frac{\omega-\omega_1}{\omega_0-\omega_1}[\mathrm{Si}((\omega-\omega_1)(t_s-t_0))-\mathrm{Si}((\omega-\omega_0)(t_s-t_0))]+\frac{\cos((\omega-\omega_1)(t_s-t_0))-\cos((\omega-\omega_0)(t_s-t_0))}{(\omega_0-\omega_1)(t_s-t_0)}$$
$$+\frac{\omega_2-\omega}{\omega_0-\omega_2}[\mathrm{Si}((\omega-\omega_1)(t_s-t_0))-\mathrm{Si}((\omega-\omega_0)(t_s-t_0))]-\frac{\cos((\omega-\omega_2)(t_s-t_0))-\cos((\omega-\omega_0)(t_s-t_0))}{(\omega_0-\omega_2)(t_s-t_0)}\Big]. \quad (19)$$

The triangle frequency distribution has three characteristic parameters instead of the two which the step function and Gaussian frequency distributions have. These parameters correspond to the bounds of the triangle and its center. The extra parameter gives an additional degree of freedom to the background fit which is able to incorporate the asymmetry of frequency distributions. This makes the triangle frequency distribution general enough to approximate a frequency distribution similar to real data.

Figure 5 shows the background for a triangular frequency distribution centered at the magic frequency with a width of 10 kHz. We can see that the form of the background looks almost identical to the Gaussian or step function backgrounds.

In figure 6 we show the background for a triangle frequency distribution centered at the magic frequency with a left bound of -10 kHz and a right bound of +30 kHz from its center. For values of $t_s$ of 20 $\mu$s and less, the background remains mostly symmetric about its center. When $t_s$ becomes large, however, the background does not obey this symmetry but instead skews to the right. This is why the step function, Gaussian, and triangle frequency distributions can befitted to the background for an asymmetric frequency distribution for approximately 20 $\mu$s, but past this point only the triangular frequency background is able to include the asymmetry.

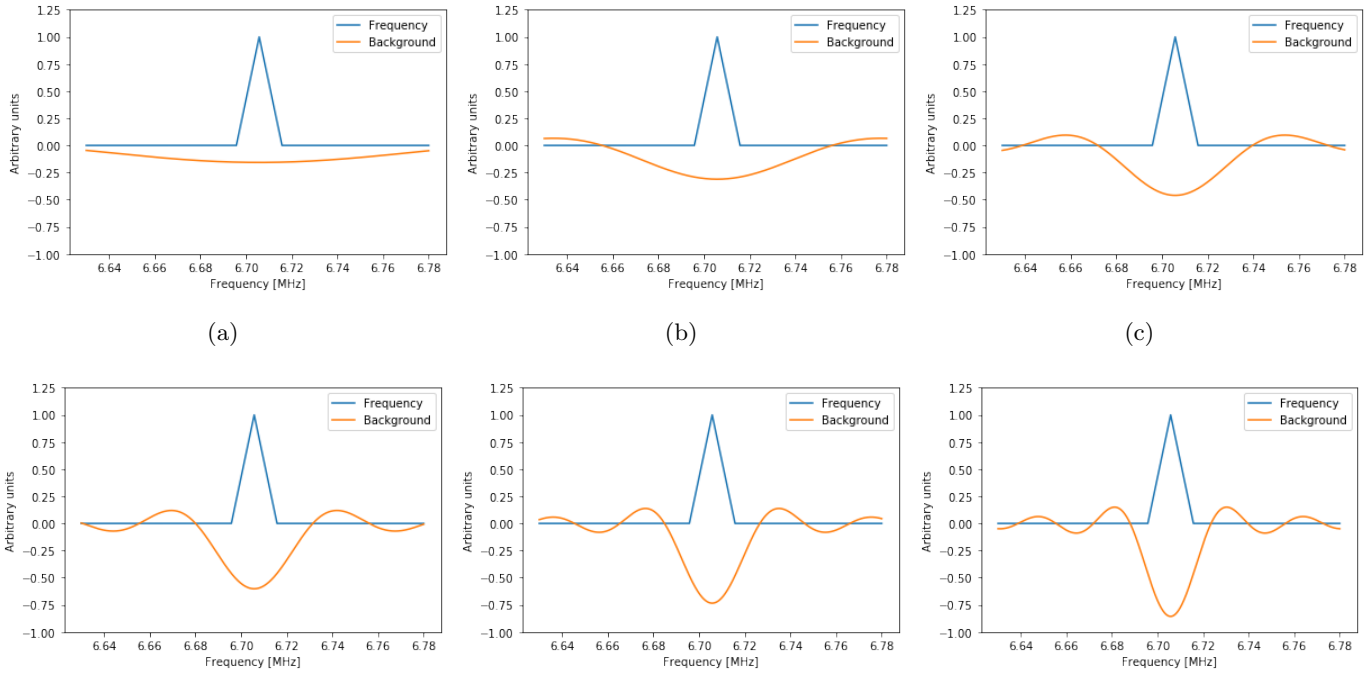


(a) (b) (c)

(d) (e) (f)

Figure 5: Background with $t_0 = 0$ $\mu$s and different values of $t_s$ for a triangular frequency distribution centered at the magic frequency and bound 10 kHz from the center. Six start times are shown: (a) 5 $\mu$s, (b) 10 $\mu$s, (c) 15 $\mu$s, (d) 20 $\mu$s, (e) 25 $\mu$s, (f) 30 $\mu$s

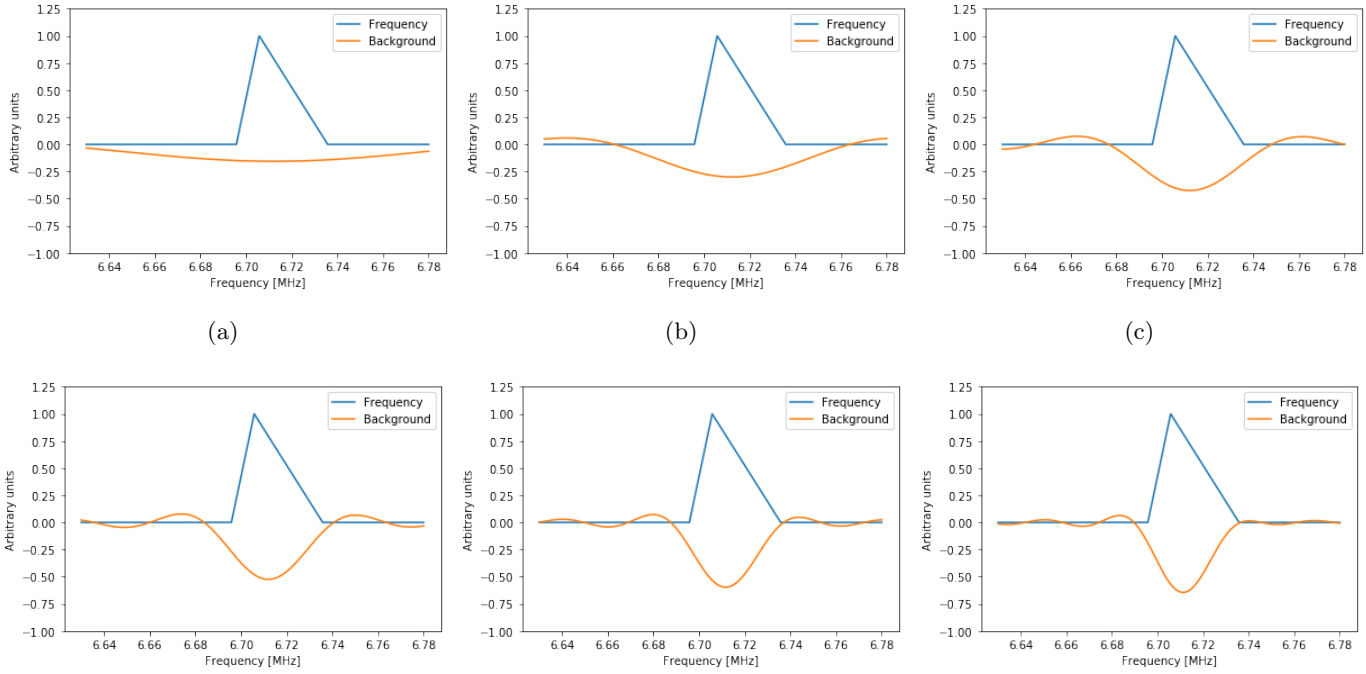


(a) (b) (c)

(d) (e) (f)

Figure 6: Background with $t_0 = 0$ $\mu$s and different values of $t_s$ for a triangular frequency distribution centered at the magic frequency left bound of -10 kHz and right bound +30 kHz from its center. Six start times are shown: (a) 5 $\mu$s, (b) 10 $\mu$s, (c) 15 $\mu$s, (d) 20 $\mu$s, (e) 25 $\mu$s, (f) 30 $\mu$s.

### 2.5 Discussion of other possible analytic forms

We have been able to derive the analytic form of the correction to the cosine Fourier transformation using four different ansatzes for the frequency distribution. There are not many frequency distributions which can be plugged into (3) to get an analytic solution. In section 4 and 5 we show how the triangular frequency distribution can be fitted to both a Gaussian and asymmetric frequency distribution backgrounds so we have succeeded in our goals.

A possible improvement over the Gaussian frequency distribution for fitting asymmetric frequency distributions would be to use a skewed-Gaussian frequency distribution defined by (37). Deriving a usable analytic form of the background for a skewed-Gaussian is very challenging since we would have to integrate it in equation(3).

An other improvement could be to use instead of a triangular frequency distribution, a higher order polygon. This complicates things however, since for each additional order of the polygon, we require an additional parameter to be fitted. The triangle frequency distribution is the most practical since it requires the least amount of parameters to fully describe the background.

## 3 Analytic background comparisons of the cosine Fourier transform

In this section we will compare how all of the analytic models for the background to the cosine Fourier transform are equivalent when $t_s$ is small, but diverge for large values of $t_s$. In appendixes B and C we show how we can Taylor expand the different analytic forms to show how these various functions are equivalent in the limit where $t_s$ is small and the frequency distribution is approximately symmetric.

### 3.1 Comparison of the delta, step, Gaussian, and triangular backgrounds

Figure 7 shows the comparison of the different analytic forms of the background to the cosine Fourier transformation derived in section 2. We normalize the background for comparison purposes.

We can see that the backgrounds almost exactly overlay with each other. It is not until late start times where the backgrounds begin to show the forms of the frequency distributions which they came from. For $t_s = 30$ $\mu$s, the delta function background is diverged from the step function, Gaussian, and triangular backgrounds. The step function, Gaussian, and triangular backgrounds behave similarly at 30 $\mu$s, however the triangular function has the special feature that it can incorporate asymmetries in the frequency distribution which can not be seen in this figure since the background is symmetric.

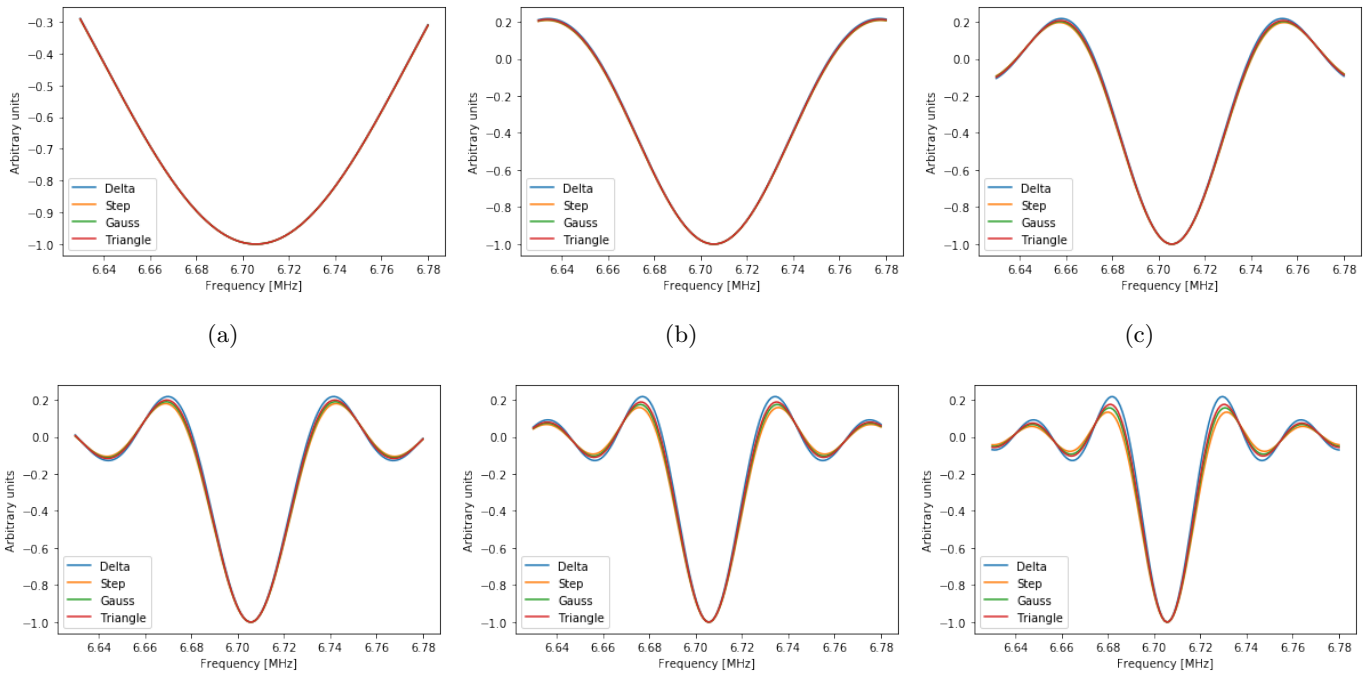


Figure 7: Background with $t_0 = 0$ $\mu$s and different values of $t_s$ for the delta function, step function, Gaussian, and triangle backgrounds used in figures [2,3,4,5]. Six start times are shown: (a) 5 $\mu$s, (b) 10 $\mu$s, (c) 15 $\mu$s, (d) 20 $\mu$s, (e) 25 $\mu$s, (f) 30 $\mu$s.

### 3.2 The background cancels the frequency distribution at late start times

In figure 8 we show the background compared to the delta function, step function, Gaussian, and triangular frequency distributions for a start time of 200 $\mu$s. The amplitude of the distributions is arbitrary so we normalize for the comparison. Note that we also do this for the delta function even though it is infinite.

We can see that using this very late start time, the background approximately matches the frequency distribution. The cosine Fourier transformation is the frequency distribution plus the correction, so for large start times the background completely cancels out the frequency distribution making it impossible to recover the complete frequency distribution.

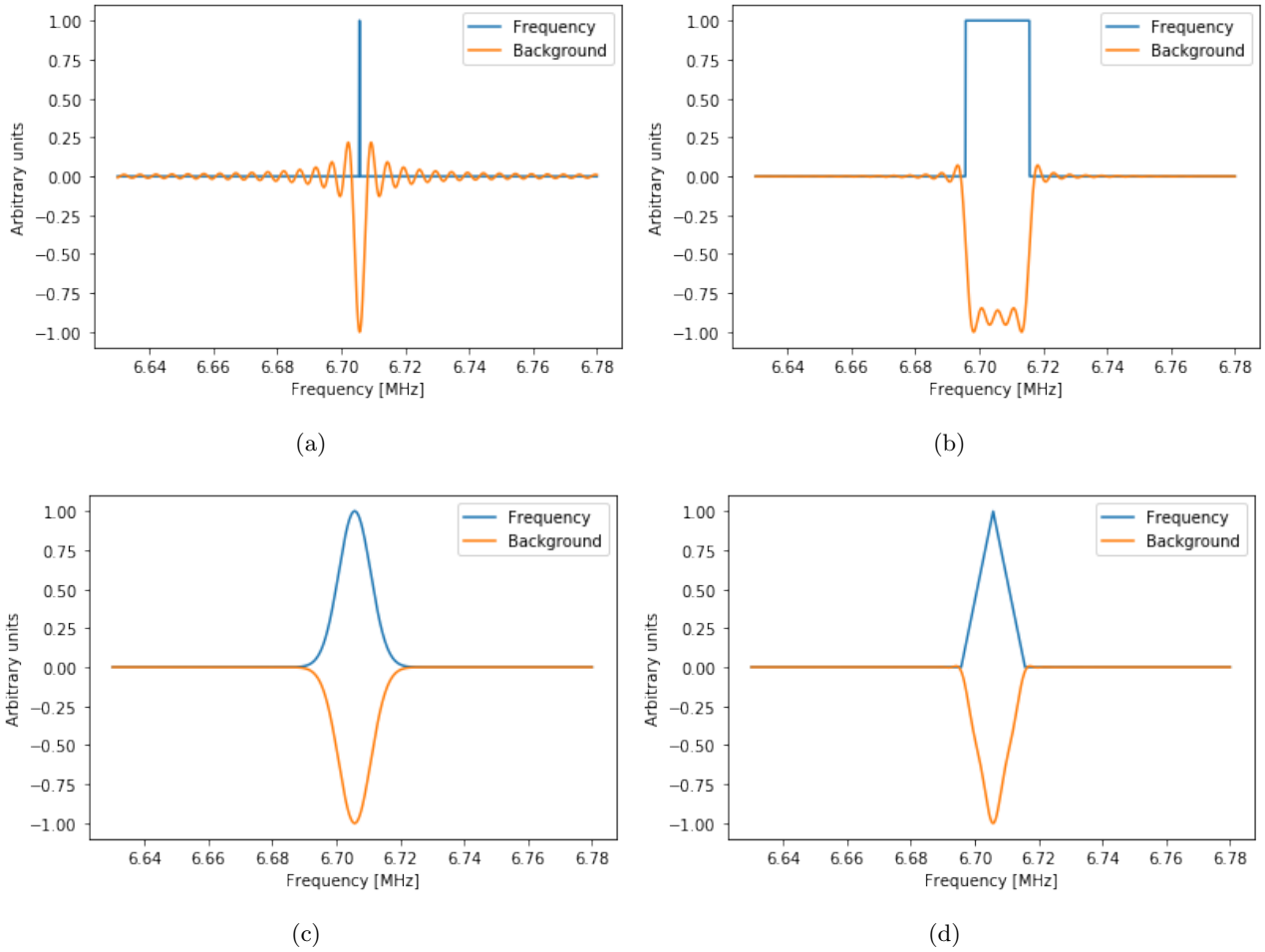


Figure 8: Background Comparison with $t_0 = 0$ $\mu$s and a large start time of $t_s = 200$ $\mu$s between Gaussian, step function, and triangular frequency distributions used in figures [2,3,4,5]. Four functions are shown: (a) Delta, (b) Step Function, (c) Gaussian, (d) triangle.

# 4 Monte Carlo fitting with a Gaussian frequency distribution

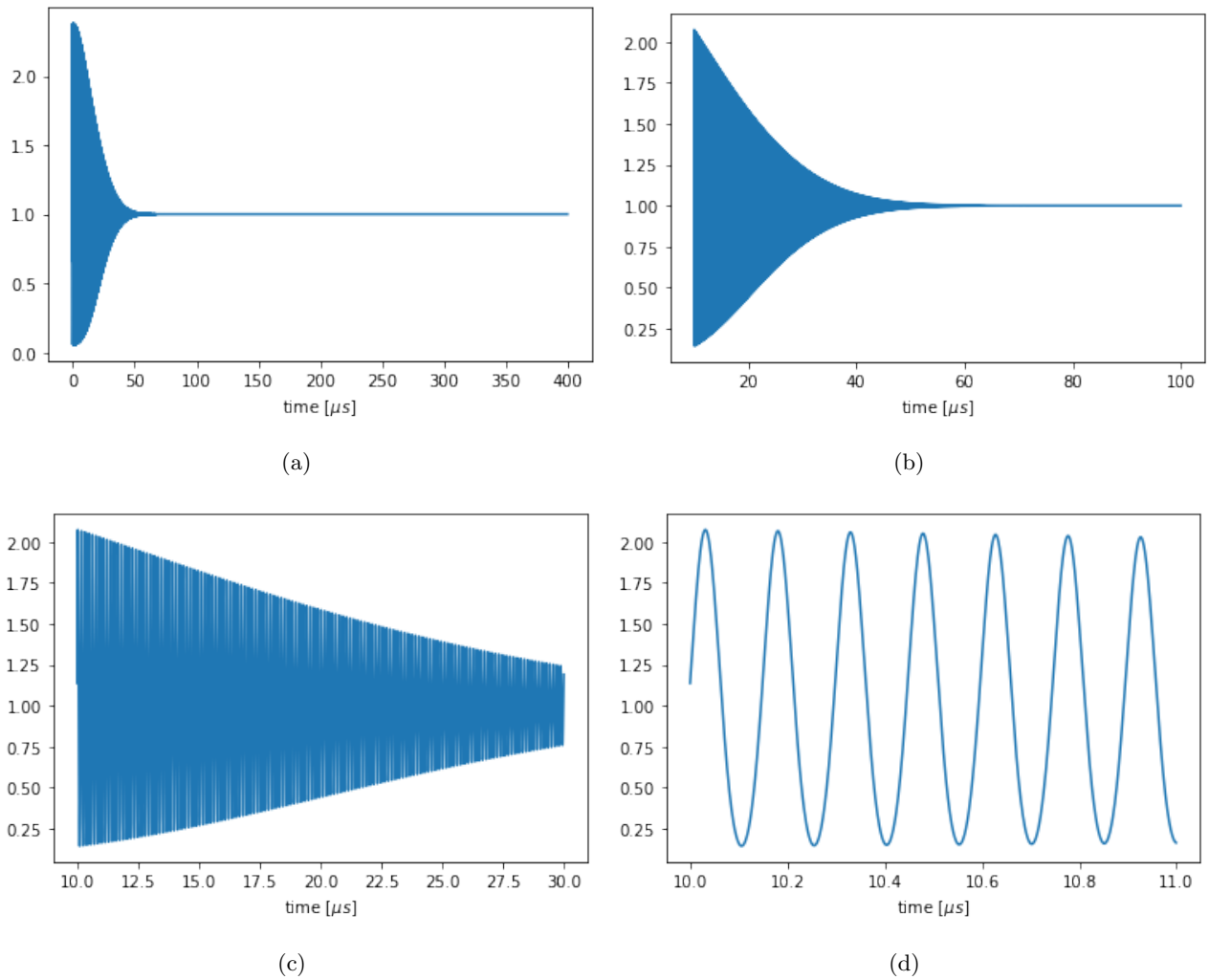


Figure 9: Fast rotation signal as a function of time generated by a Monte Carlo simulation [3]. The fast rotation signal has a Gaussian frequency distribution and longitudinal beam profile. The Frequency distribution is centered at the magic frequency with a fractional energy offset of 0.16% and the longitudinal beam profile is centered at 0 $\mu$s with a standard deviation of 25 ns. Four time intervals are shown: (a) 0-400 $\mu$s, (b) 10-100 $\mu$s, (c)10-30 $\mu$s, (d) 10-11 $\mu$s.

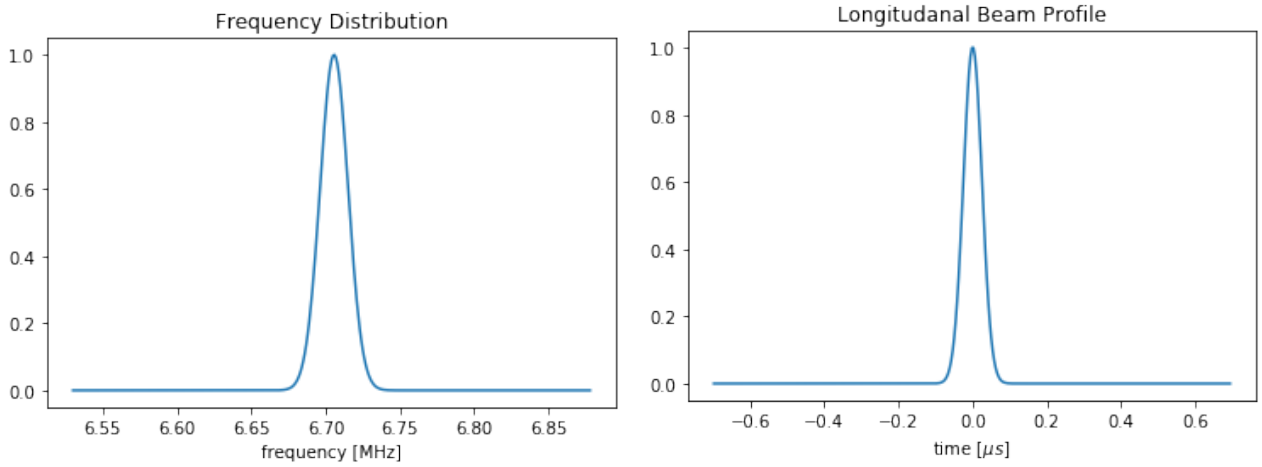


(a) (b)

Figure 10: The Gaussian frequency distribution and longitudinal beam profile used in the Monte Carlo fast rotation signal shown in figure 9. (a) Frequency distribution, (b) Longitudinal beam profile.

In figures 9 and 10 we show a Monte Carlo fast rotation signal and the frequency distribution and longitudinal beam profile used to make it. The Monte Carlo is created using the analytic form of the fast rotation signal without noise nor statistical fluctuation [3]. We use this pristine fast rotation signal to test the background fitting for the different functions.

In figure 11 we show the cosine Fourier transformation of the fast rotation signal for different values of $t_s$. In appendix A we discuss how the width of the frequency distributions limits how large $t_s$ can be and still have the approximate forms for the background to the cosine Fourier transformation be valid. For this Monte Carlo simulation, we use a frequency distribution wider than what is found in the data since we want to find the upper limits of $t_s$ that allows us to reliably recover the frequency distribution.

For large values of $t_s$, the background distorts the main peak of the cosine Fourier transformation and it will no longer resemble the actual frequency distribution. This is because by $t_s = 20$ $\mu$s the width of the main peak begins to get smaller as the background merges with it. For the small start time of $t_s = 5$ $\mu$s the background on the cosine Fourier transformation is approximately parabolic and does not interfere with the actual signal.

The background is fitted to the cosine Fourier transformation using frequencies a distance away from the minima which we specify in each figure. The fitted background is subtracted from the cosine Fourier transformation to recover the original frequency distribution. This is the simplest way of recovering the frequency, but we can use the full Fourier method for more accuracy [1]. The results of our analysis underperforms what would be obtained using the full method.

**Important note**: In this note the E-field correction is calculated using the linear approximation [1]. For Monte Carlo simulations the field index is arbitrary so we use a value of n = 0.1075 which to match the Run-1 60-hour data set.

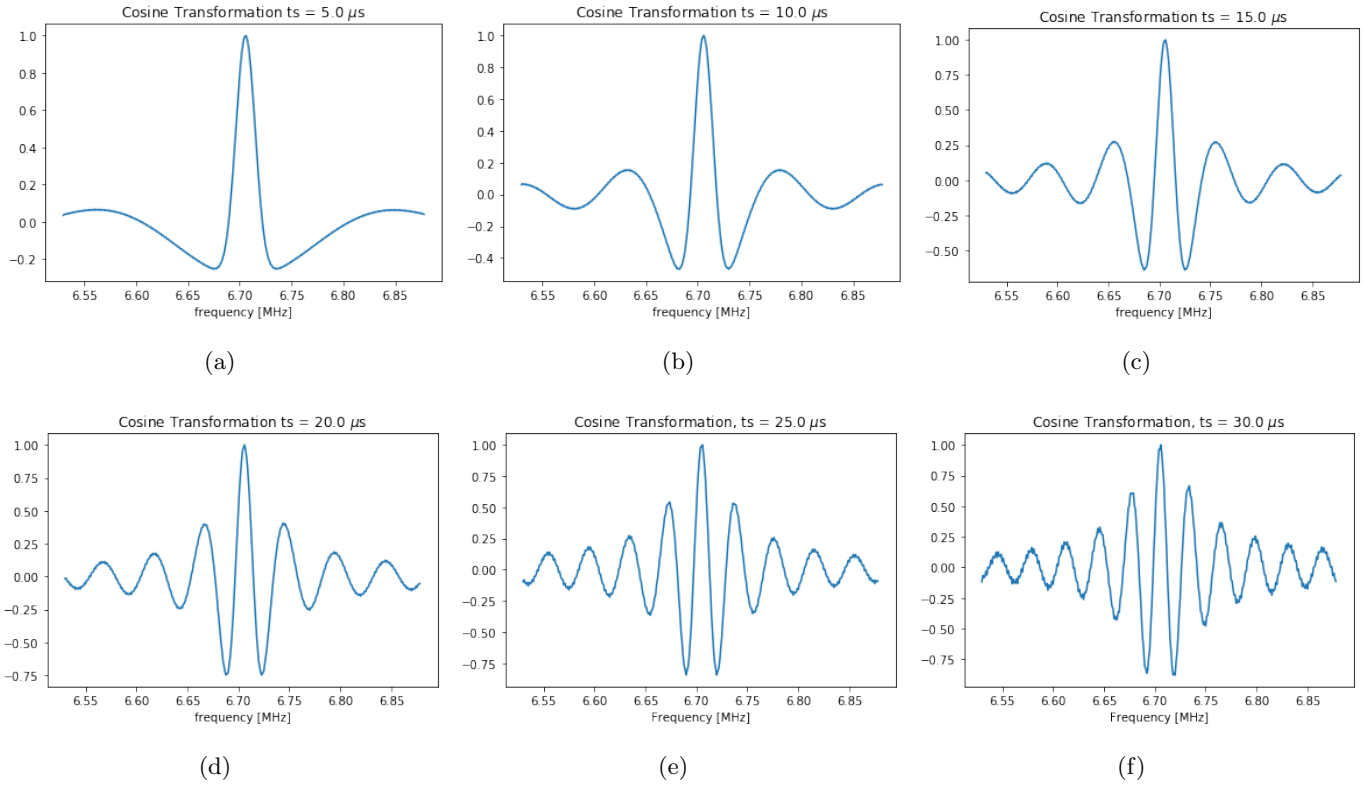


Figure 11: cosine Fourier transformation of the Monte Carlo in figure 9 using the correct value of $t_0$ with different values of $t_s$. Six start times are shown: (a) 5 $\mu$s, (b) 10 $\mu$s, (c) 15 $\mu$s, (d) 20 $\mu$s, (e) 25 $\mu$s, (f) 30 $\mu$s.

### 4.1 polynomial

We can Taylor expand any of the analytic forms of the background which we derived, so we know that the background can be fitted with a polynomial for small start times. In the following equation we show how we can Taylor expand the sine function around $\omega = \omega_0$ when $|(\omega - \omega_0)(t_s - t_0)| \ll 1$:

$$\begin{aligned}\Delta(\omega) &= \frac{1}{\pi}\frac{\sin[(\omega-\omega_0)(t_s-t_0)]}{(\omega-\omega_0)} \\ &= \frac{1}{\pi}\frac{1}{(\omega-\omega_0)}\sum_{n=0}^{\infty}\frac{(-1)^n[(\omega-\omega_0)(t_s-t_0)]^{2n+1}}{(2n+1)!} = \frac{(t_s-t_0)}{\pi}\sum_{n=0}^{\infty}\frac{(-1)^n[(\omega-\omega_0)(t_s-t_0)]^{2n}}{(2n+1)!} \\ &= \frac{(t_s-t_0)}{\pi}\Big(1-\frac{[(\omega-\omega_0)(t_s-t_0)]^2}{3!}+\frac{[(\omega-\omega_0)(t_s-t_0)]^4}{5!}-\frac{[(\omega-\omega_0)(t_s-t_0)]^6}{7!}+...\Big).\end{aligned} \tag{20}$$

This is the simplest way of fitting the background since it does not require any knowledge of the shape of the background because each coefficient of the polynomial is fitted without having to give any initial values.

In appendix A we discuss how when $t_s$ is small the background is approximately parabolic. For this small start time, we only need a degree 2 polynomial to fit the background. If we use a higher order polynomial then we can use some larger values of $t_s$.

We show in figure 12 that the background can be fitted with a degree 6 polynomial for $t_s = 5$ $\mu$s. There does not seem to be any downside to using more orders of the polynomial, so we use 6 terms of the polynomial

which is more than enough.

Figure 13 shows that by 10 $\mu$s, the background is too highly-nonlinear and not of polynomial form to be fitted. To skip scraping we will have to use more sophisticated fit functions, however the polynomial fit is more than sufficient to skip the beam-line positron contamination of the muon beam

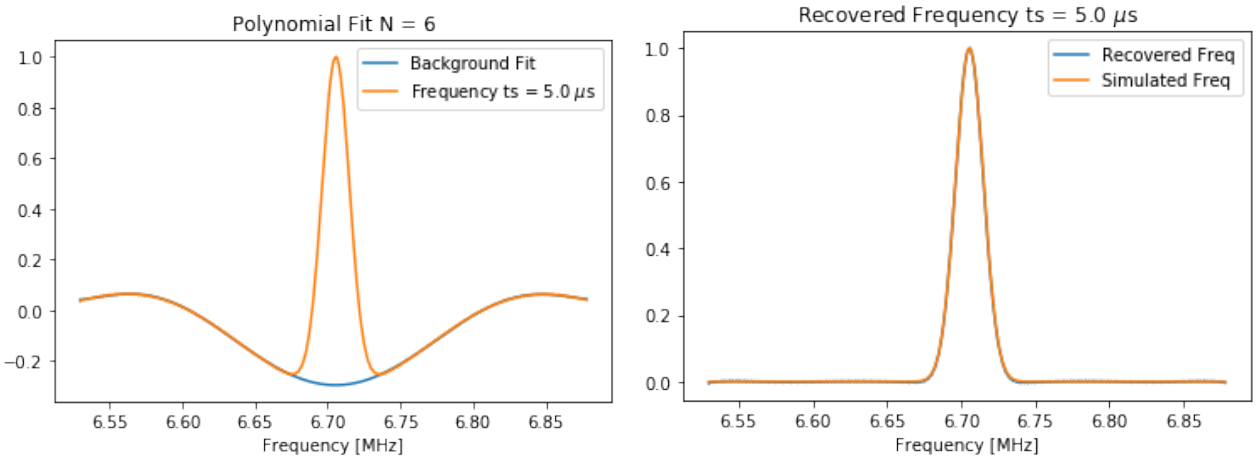


(a) (b)

Figure 12: Fitting the background with a polynomial fit of degree 6 with $t_s = 5$ $\mu$s fitting 0.5 kHz away from minima. (a) Fitted cosine Fourier transformation (b) Recovered Frequency Distribution.

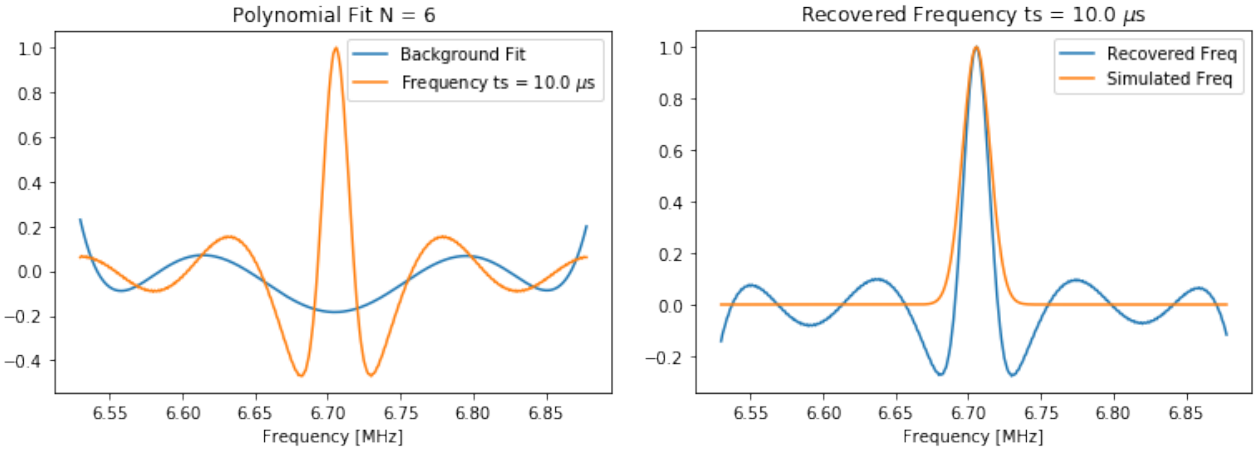


(a) (b)

Figure 13: Fitting the background with a polynomial fit of degree 6 with $t_s = 10$ $\mu$s fitting 0.5 kHz away from minima. (a) Fitted cosine Fourier transformation, $C_E$ = -378.04 ppb (b) Recovered Frequency Distribution, $C_E$ = -359.52 ppb.

## 4.2 sinc

We showed in section 2.1 that we can approximate the frequency background using a sinc function in equation (6). This enables us to fit the background outside the signal with a sinc function. The amplitude of the background is arbitrary so we fit the background as the following:

$$\Delta(\omega) = -A\,\mathrm{sinc}[(\omega - \omega_0)t], \tag{21}$$

where the parameters A, $\omega_0$, and t are fitted to match the distribution. The parameter t represents $t_s - t_0$. We could include an additive constant term to the background fit as well, but it does not make any difference on the fit as it will be fitted to nearly zero. We therefore do not included an additive constant for any of our fit functions.

Figure 14 shows the sinc background fit for $t_s = 5$ $\mu$s. This fits the background well with a $C_E$ difference of only 13.42 ppb. For large values of $t_s$, the background cannot be fitted as well. We show in figure 15 that the sinc function being fitted to the background for $t_s = 30$ $\mu$s which yields a large $C_E$ difference of 222.2 ppb. The sinc function will outperform the polynomial fit, however still falters for values of $t_s$ greater than 15 $\mu$s.

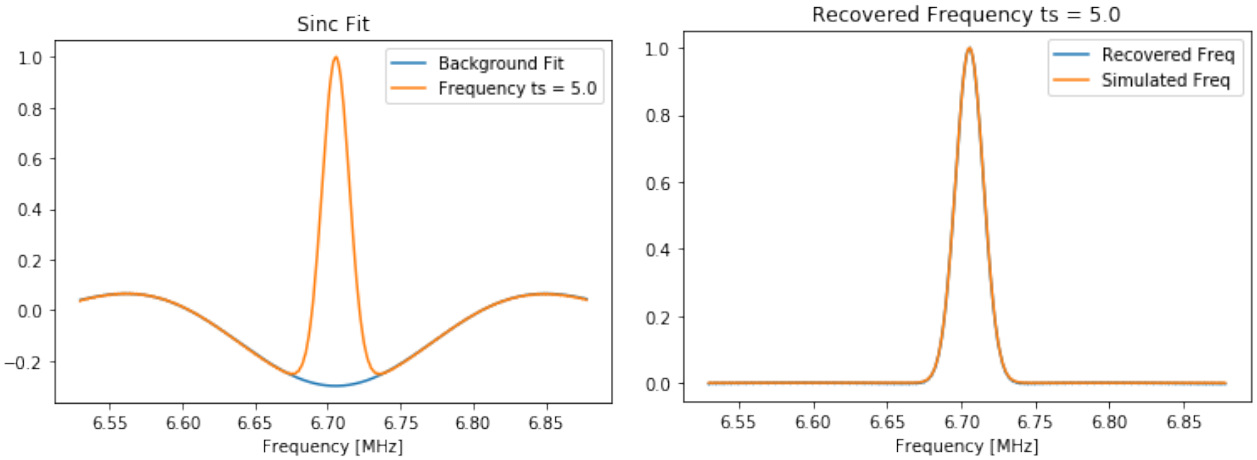


(a) (b)

Figure 14: Fitting the background with a sinc function with $t_s = 5$ $\mu$s fitting 2.0 kHz away from the minima. (a) Fitted cosine Fourier transformation, $C_E$ = -378.04 ppb (b) Recovered Frequency Distribution, $C_E$ = -379.70 ppb.

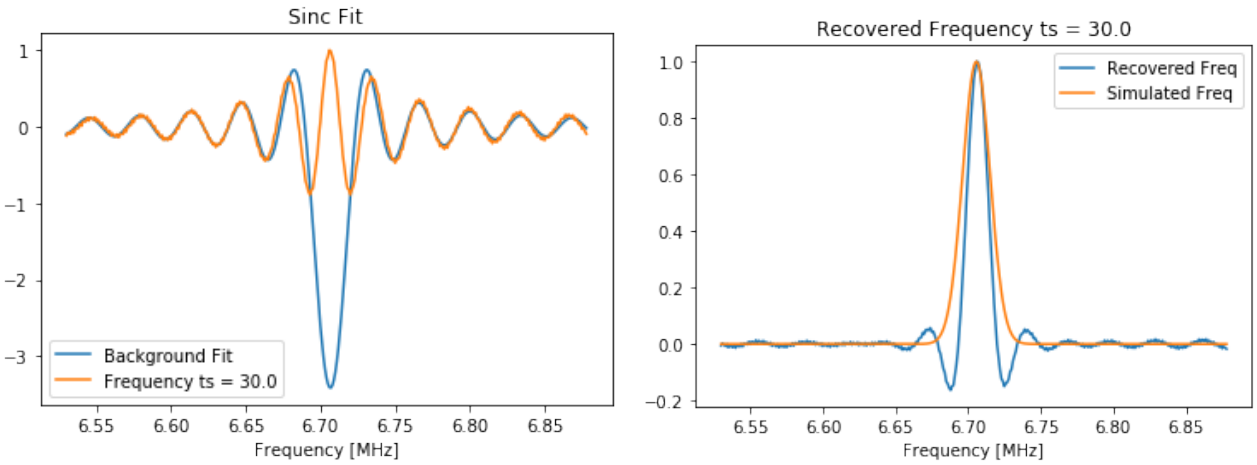


(a) (b)

Figure 15: Fitting the background with a sinc function with $t_s = 30$ $\mu$s fitting 2.0 kHz away from the minima. (a) Fitted cosine Fourier transformation, $C_E$ = -378.04 ppb (b) Recovered Frequency Distribution, $C_E$ = -167.82 ppb.

### 4.3 Si

We showed in section 2.2 to be Si functions of the form in equation (22). With an arbitrary amplitude we approximate the form of the background to be:

$$\Delta(\omega) = -A\big[\,\mathrm{Si}((\omega-\omega_1)t) - \mathrm{Si}((\omega-\omega_2)t)\big], \tag{22}$$

where the fit parameters A, $\omega_1$, $\omega_2$, and t. We see in figure 16 that for $t_s = 5$ $\mu$s the background is fitted very well with a difference in $C_E$ of only 1.66 ppb. For $t_s = 15$ $\mu$s as shown in figure 17, we are still able to fit the background using with this analytic form yielding only a small $C_E$ difference of 8.35 ppb. For $t_s = 30$ $\mu$s, the Si function fits the background decently, but there is still a large $C_E$ difference of 154.0 ppb since the frequency distribution includes negative values.

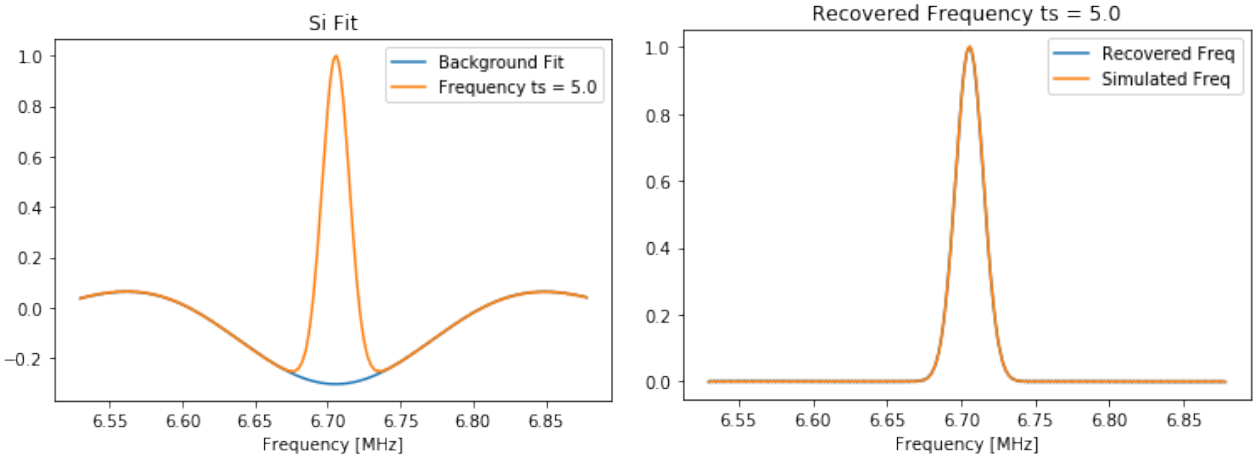


(a) (b)

Figure 16: Fitting the background with Si functions with $t_s = 5$ $\mu$s fitting 2.0 kHz away from the minima. (a) Fitted cosine Fourier transformation, $C_E$ = -378.04 ppb (b) Recovered Frequency Distribution, $C_E$ = -379.70 ppb.

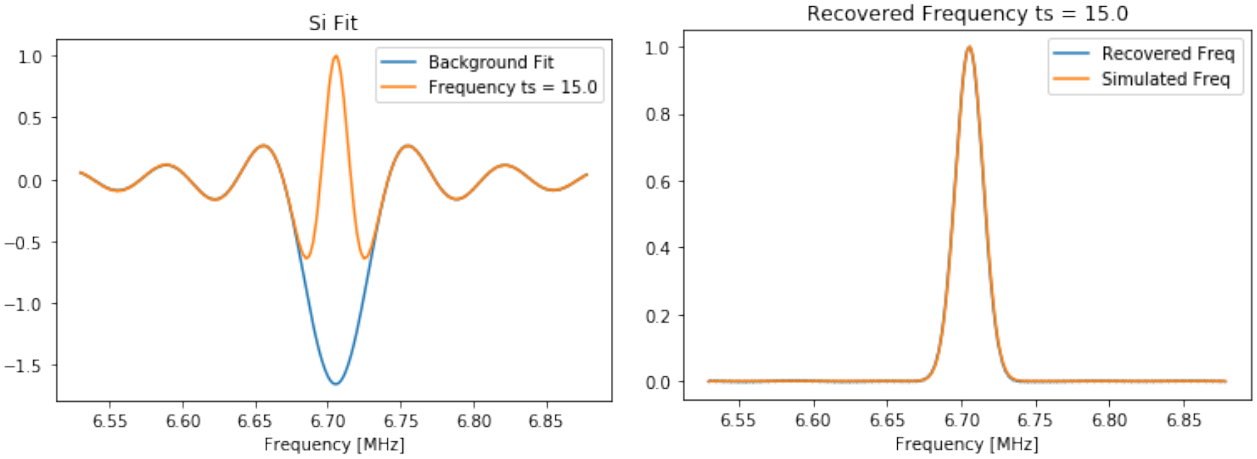


(a) (b)

Figure 17: Fitting the background with Si functions with $t_s = 15$ $\mu$s fitting 2.0 kHz away from the minima. (a) Fitted cosine Fourier transformation, $C_E$ = -378.04 ppb (b) Recovered Frequency Distribution, $C_E$ = -369.68 ppb.

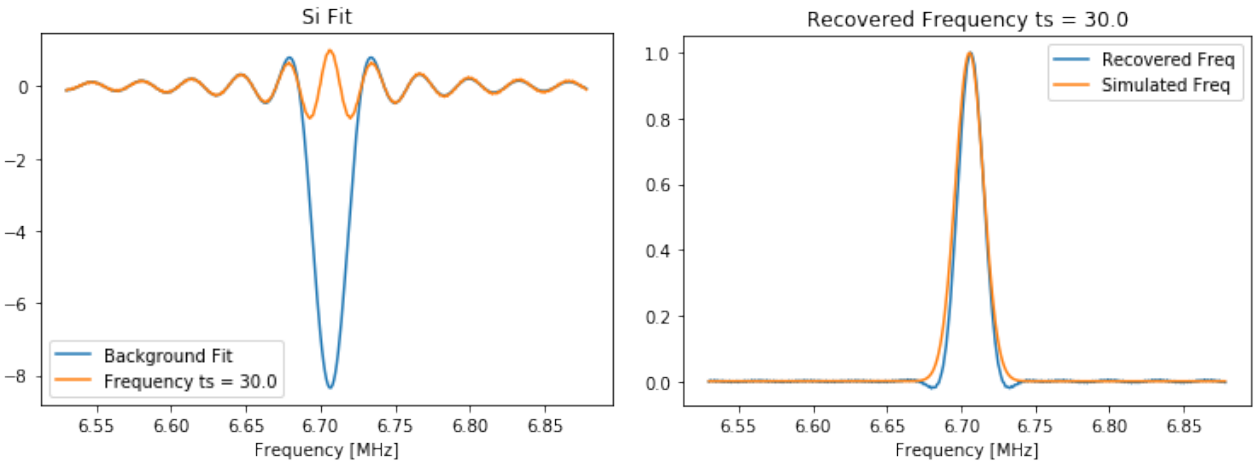


(a) (b)

Figure 18: Fitting the background with a Si functions with $t_s = 30$ $\mu$s fitting 2.0 kHz away from the minima. (a) Fitted cosine Fourier transformation, $C_E$ = -378.04 ppb (b) Recovered Frequency Distribution, $C_E$ = -224.03 ppb.

### 4.4 erfi

We derive in section 2.3 that the background for a Gaussian frequency distribution takes the form of equation (16). With an arbitrary amplitude we use the fit function of the following form:

$$\Delta(\omega) = -Ae^{\frac{-(\omega-\omega_0)^2}{2\sigma^2}} \text{Im}\Big\{ \text{erfi}\,(\frac{\omega - \omega_0 + i\sigma^2 t}{\sqrt{2\sigma^2}})\Big\}, \tag{23}$$

and we fit for the parameters A, $\sigma$, $\omega_0$, and t. Figure 19 shows that the background can be fitted well using the erfi function for $t_s = 5$ $\mu$s yielding a $C_E$ difference of only 1.66 ppb from the known answer. Unlike the other background forms, we shown in figure 20 that we can fit the background using the erfi function for values all the way up to $t_s = 30$ $\mu$s without problems. The difference in E-field correction at $t_s = 30$ $\mu$s is only 7.35 ppb, so we succeeded in our goal to use a value of $t_s$ large enough to skip scraping for this Gaussian Monte Carlo.

We should not be too surprised that we were able to fit the background all the way up to $t_s = 30$ $\mu$s since we are using the exact analytic form of the background for a Gaussian frequency distribution, so we are not making any approximations in the form of the background.

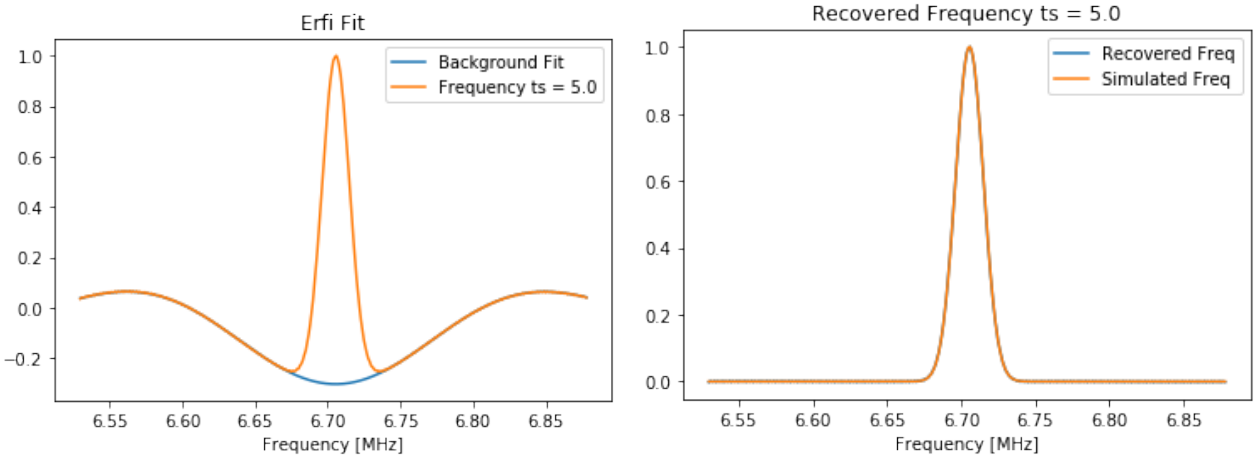


(a) (b)

Figure 19: Fitting the background with a erfi function with $t_s = 5$ $\mu$s fitting 2.5 kHz away from the minima. (a) Fitted cosine Fourier transformation, $C_E$ = -378.04 ppb (b) Recovered Frequency Distribution, $C_E$ = -379.70 ppb.

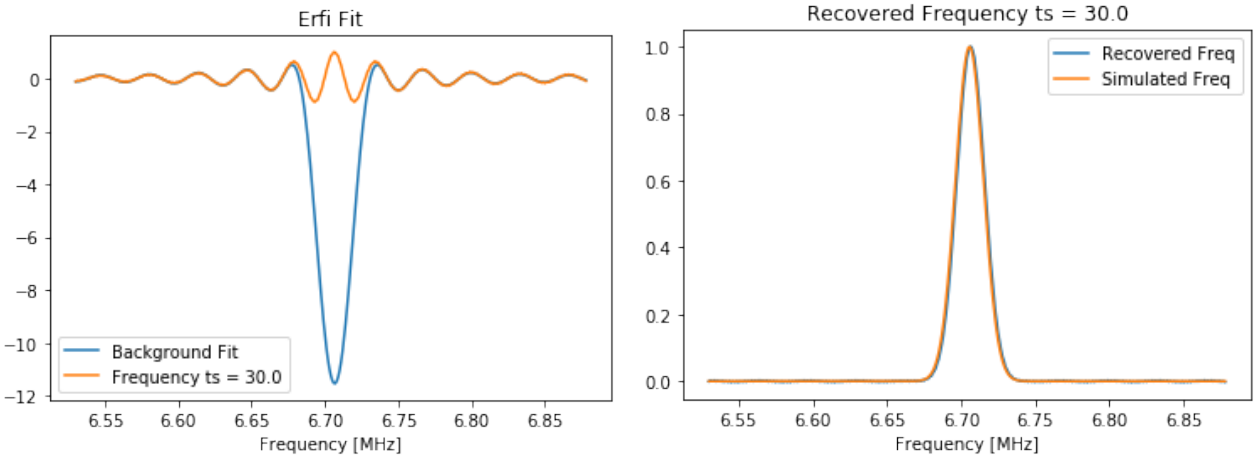


(a) (b)

Figure 20: Fitting the background with a erfi function of degree 6 with $t_s = 30$ $\mu$s fitting 2.5 kHz away from the minima. (a) Fitted cosine Fourier transformation, $C_E$ = -378.04 ppb (b) Recovered Frequency Distribution, $C_E$ = -385.39 ppb.

### 4.5 Triangular

In section 2.4 we showed that a triangular frequency distribution produces a frequency background of the form in equation (19). When we include an arbitrary amplitude we obtain the following form of the background:

$$\Delta(\omega) = -A\Big[\frac{\omega-\omega_1}{\omega_0-\omega_1}[\mathrm{Si}((\omega-\omega_1)t) - \mathrm{Si}((\omega-\omega_0)t)] + \frac{\cos((\omega-\omega_1)t) - \cos((\omega-\omega_0)t)}{(\omega_0-\omega_1)t} + \frac{\omega_2-\omega}{\omega_0-\omega_2}[\mathrm{Si}((\omega-\omega_1)t) - \mathrm{Si}((\omega-\omega_0)t)] - \frac{\cos((\omega-\omega_2)t) - \cos((\omega-\omega_0)t)}{(\omega_0-\omega_2)t}\Big], \quad (24)$$

where the parameters A, $\omega_1$, $\omega_2$, $\omega_0$, and t are fitted to the background. In figure 21 we show that for $t_s = 5$ $\mu$s, the background is fitted well with a $C_E$ difference of only 0.321 ppb. For $t_s = 15$ $\mu$s as shown in figure 22, the background can still be fitted using the triangle function with a $C_E$ difference of 17.77 ppb. When we use a very late start time like $t_s = 30$ $\mu$s shown in figure 23, the triangle function fits the background decently, however we still get a large $C_E$ difference of 97.22 ppb. This is similar to what happened when we used the Si function.

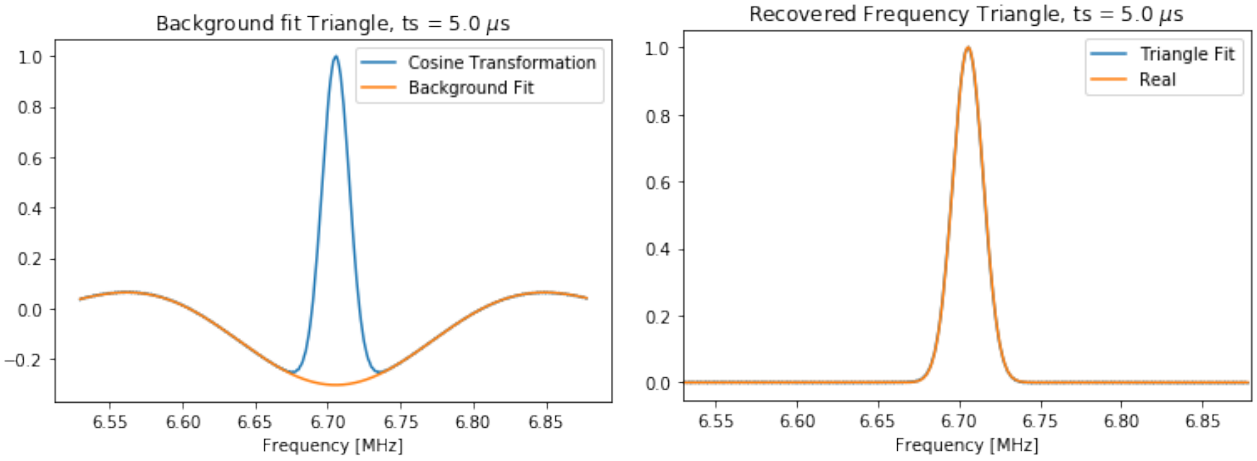


(a) (b)

Figure 21: Fitting the background with the triangular background with $t_s = 5$ $\mu$s fitting 2.0 kHz away from the minima. (a) Fitted cosine Fourier transformation, $C_E$ = -378.04 ppb (b) Recovered Frequency Distribution, $C_E$ = -378.35 ppb.

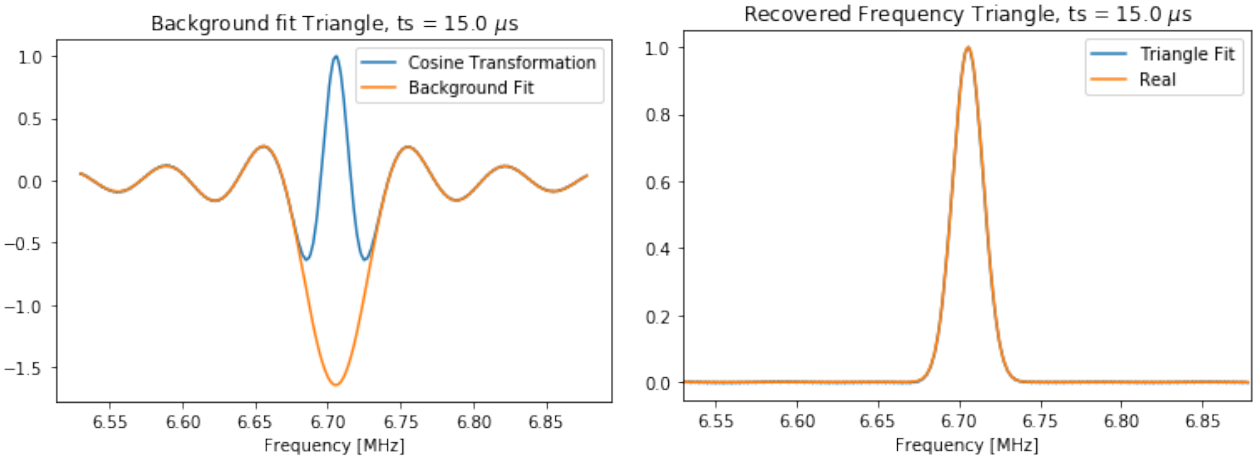


(a) (b)

Figure 22: Fitting the background with the triangular background with $t_s = 15$ $\mu$s fitting 2.0 kHz away from the minima. (a) Fitted cosine Fourier transformation, $C_E$ = -378.04 ppb (b) Recovered Frequency Distribution, $C_E$ = -360.27 ppb.

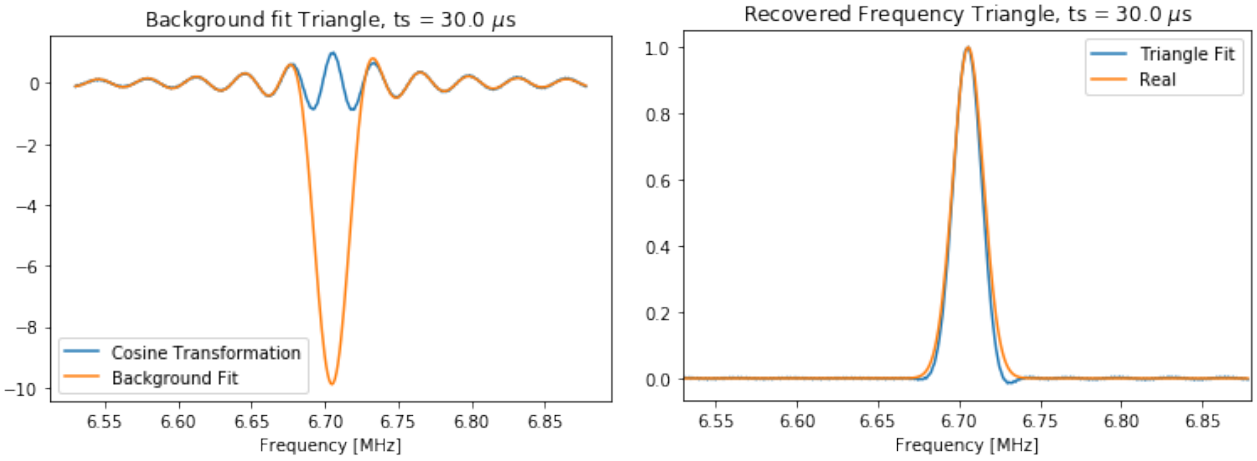


(a) (b)

Figure 23: Fitting the background with the triangular background with $t_s$ = 30 $\mu$s fitting 2.0 kHz away from the minima. (a) Fitted cosine Fourier transformation, $C_E$ = -378.04 ppb (b) Recovered Frequency Distribution, $C_E$ = -280.82 ppb.

## 5 Monte Carlo fitting with an asymmetric frequency distribution

We also want to test if the frequency background can be fitted using an asymmetric frequency distribution. In figure 24 we show how the recovered frequency distribution for the Run-1 60-hour data set is asymmetric. We will use the asymmetric frequency distribution shown in figure 24 which is used to generate the fast rotation signal with a realistic longitudinal beam profile shown in figure 25.

This Monte Carlo also has statistical uncertainty with it which makes the cosine Fourier transformation have a lot of statistical fluctuations when $t_s$ is large. This is because the muon beam is completely debunched around the ring by 100 $\mu$s of the fast rotation signal, so skipping a large part of the fast rotation signal where the muon beam has not yet debunched severely limits the statistics of the cosine Fourier transform. This can be seen in figure 26 since when $t_s$ is 15 $\mu$s or less the cosine Fourier transformation is smooth, but for larger values of $t_s$ there are large statistical fluctuations.

We are now using an asymmetric frequency distribution, so we do not optimize for $t_0$ for each values of $t_s$. We instead find $t_0$ once for $t_s$ = 4 $\mu$s and then fix the value.

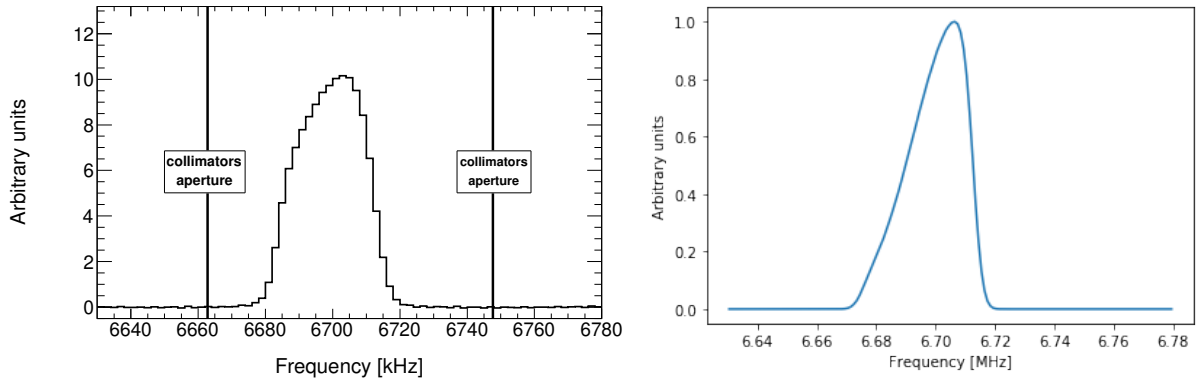


(a) (b)

Figure 24: (a) This is the recovered frequency distribution of the Run-1 60-hour data set (b) a similarly asymmetric frequency distribution to be used in a Monte Carlo simulation.

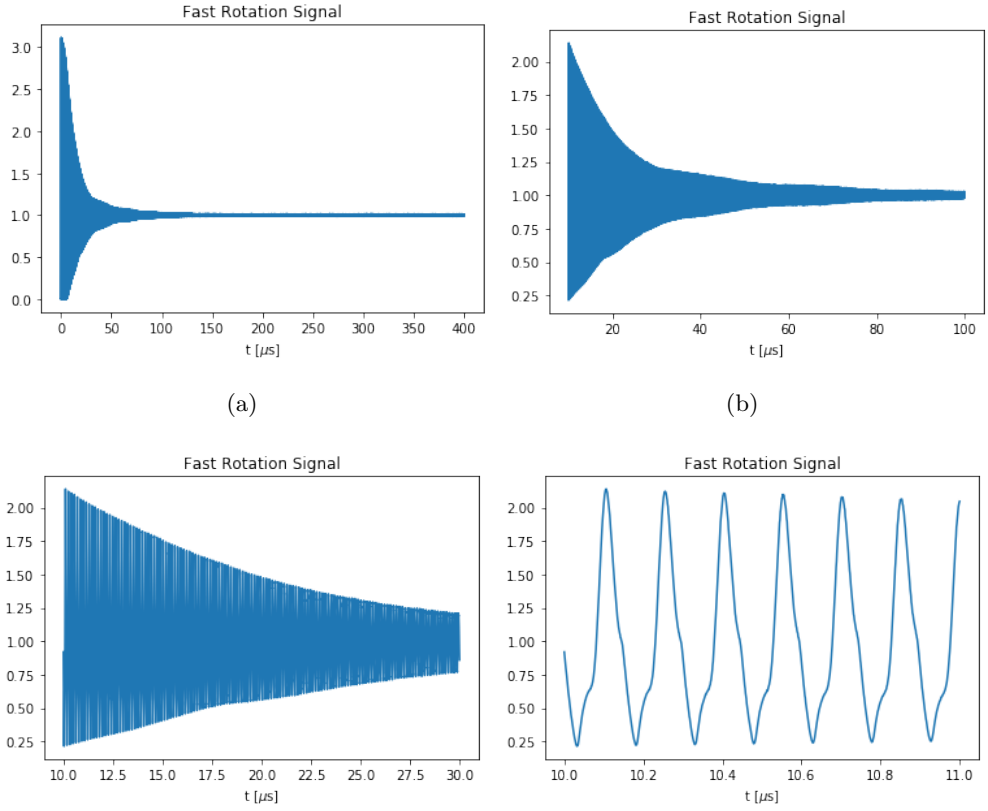


(a) (b)

(c) (d)

Figure 25: A fast rotation signal generated using a Monte Carlo simulation [4]. Four time intervals are shown: (a) 0-400 $\mu$s, (b) 10-100 $\mu$s, (c)10-30 $\mu$s, (d) 10-11 $\mu$s.

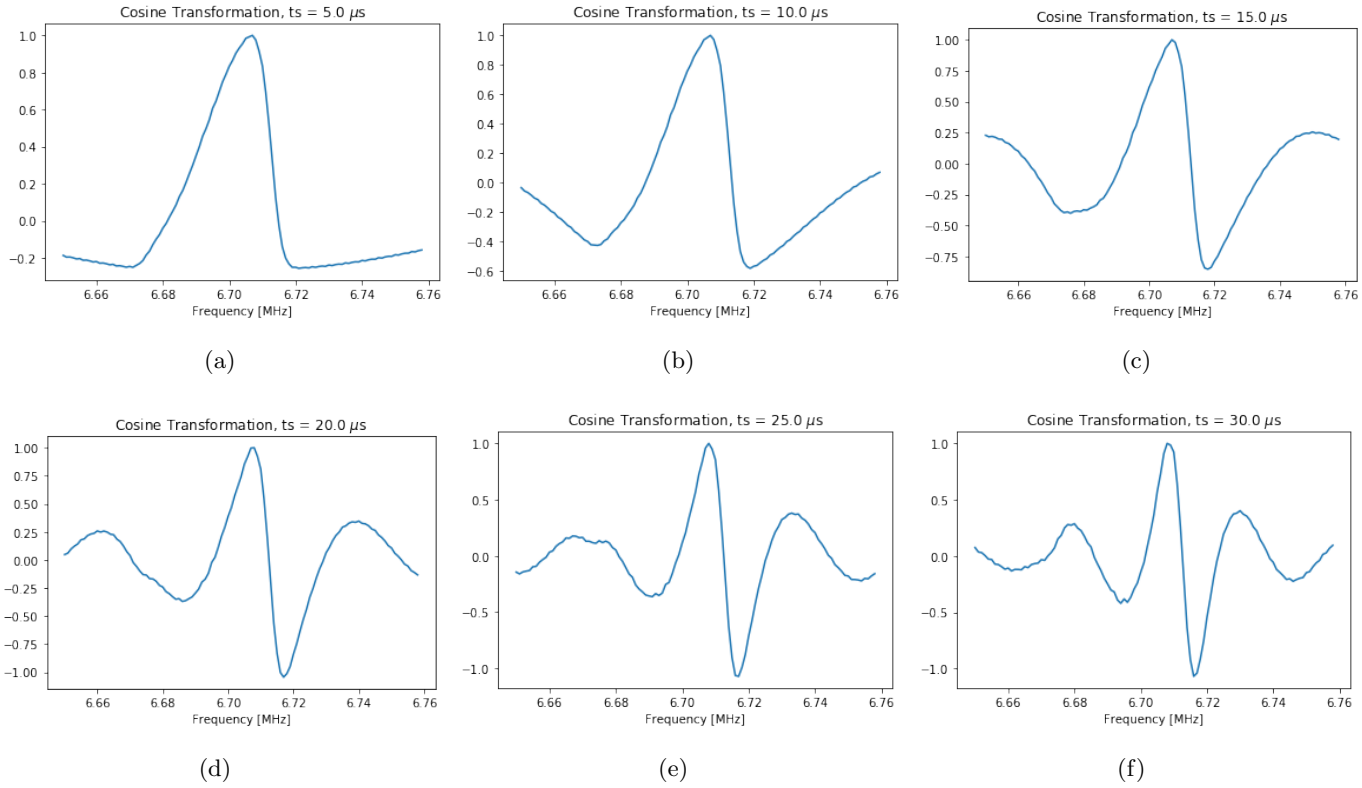


(a) (b) (c)

(d) (e) (f)

Figure 26: cosine Fourier transformation of the Monte Carlo simulation from figure 25 using a fixed value of $t_0$ and different values of $t_s$. Six start times are shown: (a) 5 $\mu$s, (b) 10 $\mu$s, (c) 15 $\mu$s, (d) 20 $\mu$s, (e) 25 $\mu$s, (f) 30 $\mu$s.

## 5.1 Fit comparison

We show in figure 27 how the background can be fitted for using any of the fit functions for $t_s = 5$ $\mu$s. When we use a larger start time like $t_s = 15$ $\mu$s shown in figure 28, the polynomial can no longer fit the background since it is highly non-linear and no longer takes a polynomial form. The sinc function is also ineffective at fitting the background because approximating the frequency distribution to be a delta function is no longer valid. For $t_s = 25$ $\mu$s shown in figure 29, the erfi and the Si functions can no longer be fitted to the background either since the approximation that the background is a Gaussian or a step function is no longer valid since neither a Gaussian or a step function can account for asymmetries. We see in figure 30 that the triangular background fit, on the other hand, can fitted to the background all the way up to $t_s = 30$ $\mu$s since the triangular background can account for asymmetries in the frequency distribution. For $t_s = 30$ $\mu$s, however, large statistical fluctuations limit the ability to reasonably recover the complete frequency distribution. While the background can be fitted decently, we show in the next section how the recovered E-field cannot be properly recovered.

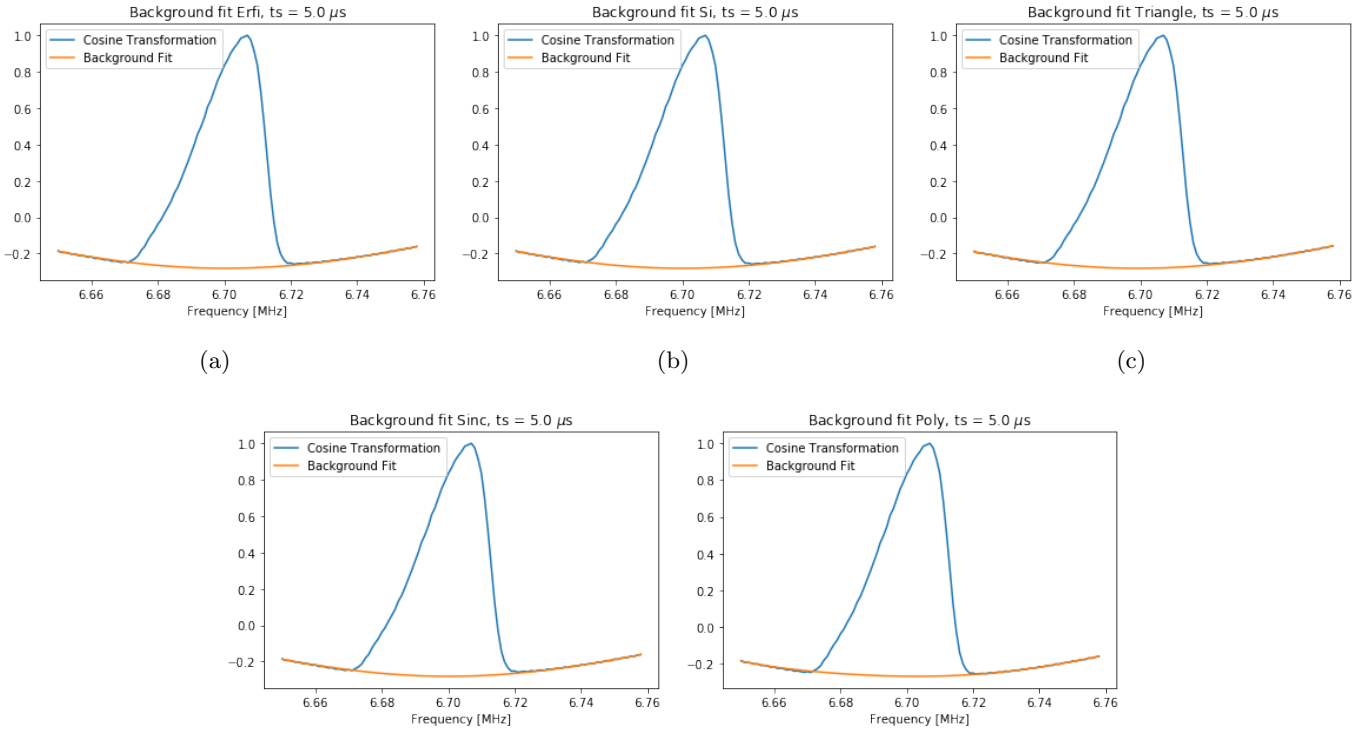


Figure 27: Fitting the frequency background 1.5 kHz away from the minima with $t_s = 5$ $\mu$s. The five fit functions are shown: (a) erfi, (b) Si, (c) triangle, (d) sinc, (e) poly.

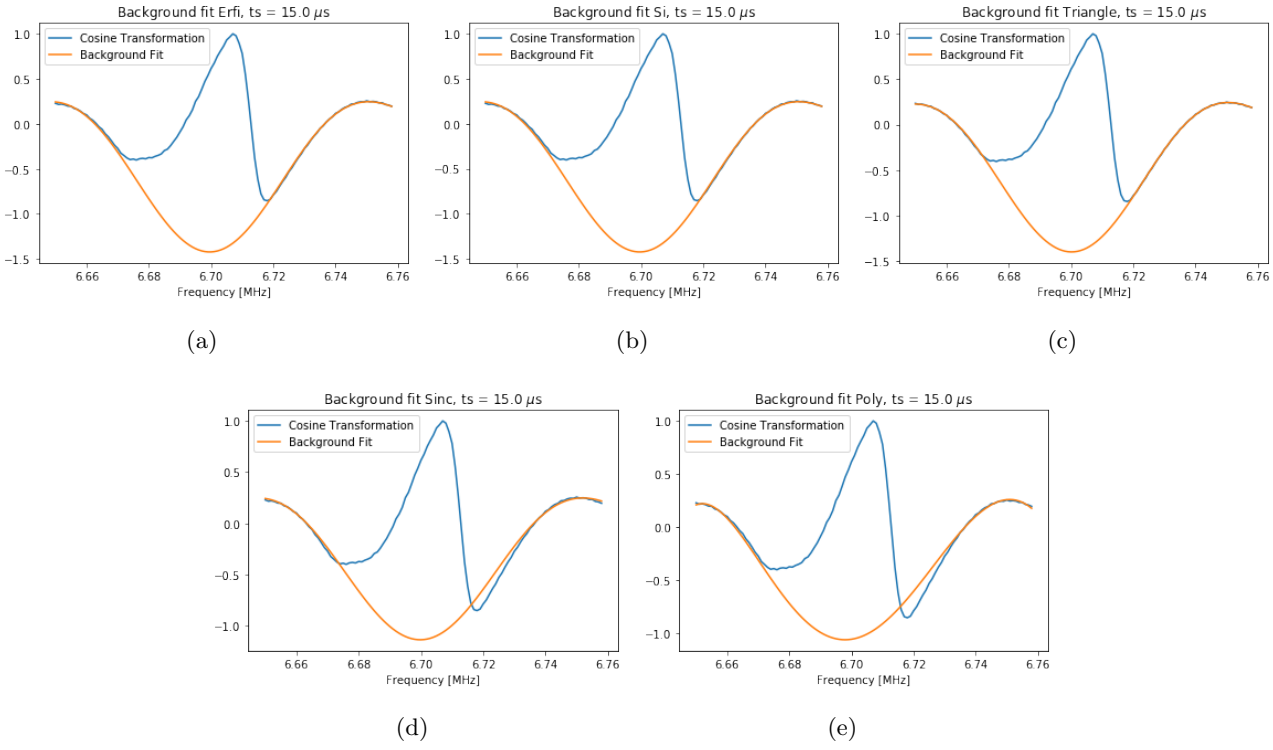


Figure 28: Fitting the frequency background 1.5 kHz away from the minima with $t_s = 15$ $\mu$s. The five fit functions are shown: (a) erfi, (b) Si, (c) triangle, (d) sinc, (e) poly

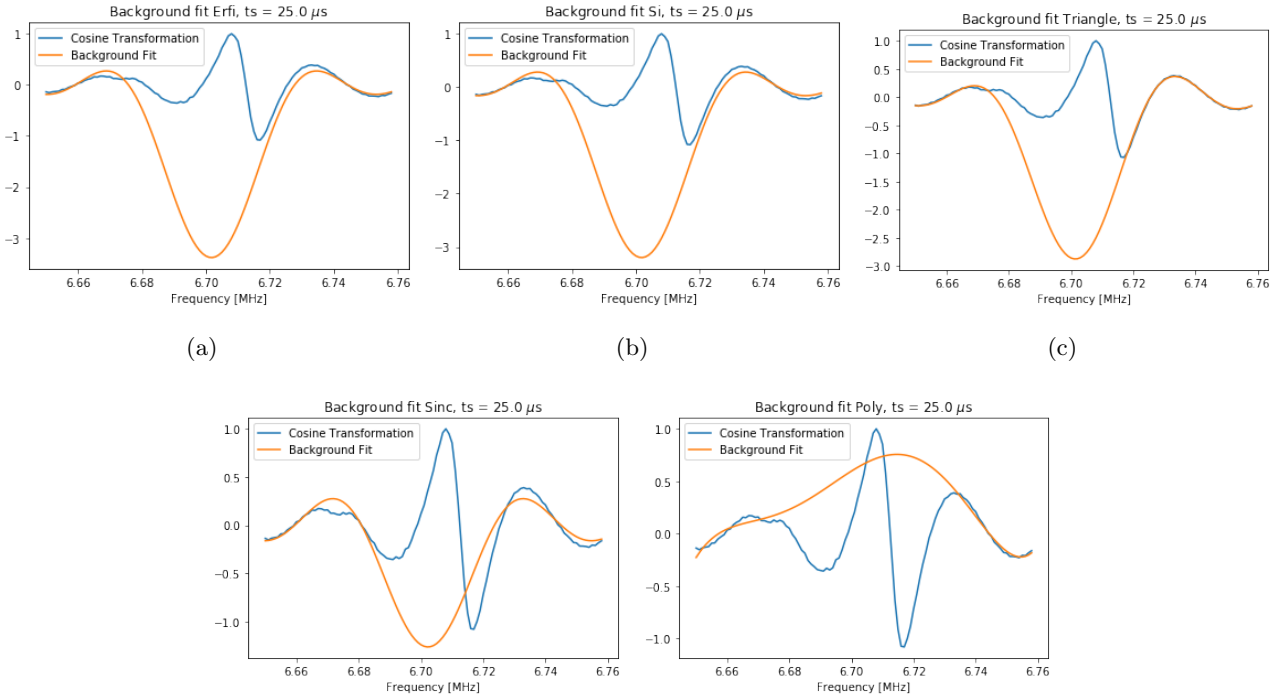


(a) (b) (c)

(d) (e)

Figure 29: Fitting the frequency background 1.5 kHz away from the minima with $t_s = 25$ $\mu$s. The five fit functions are shown: (a) erfi, (b) Si, (c) triangle, (d) sinc, (e) poly.

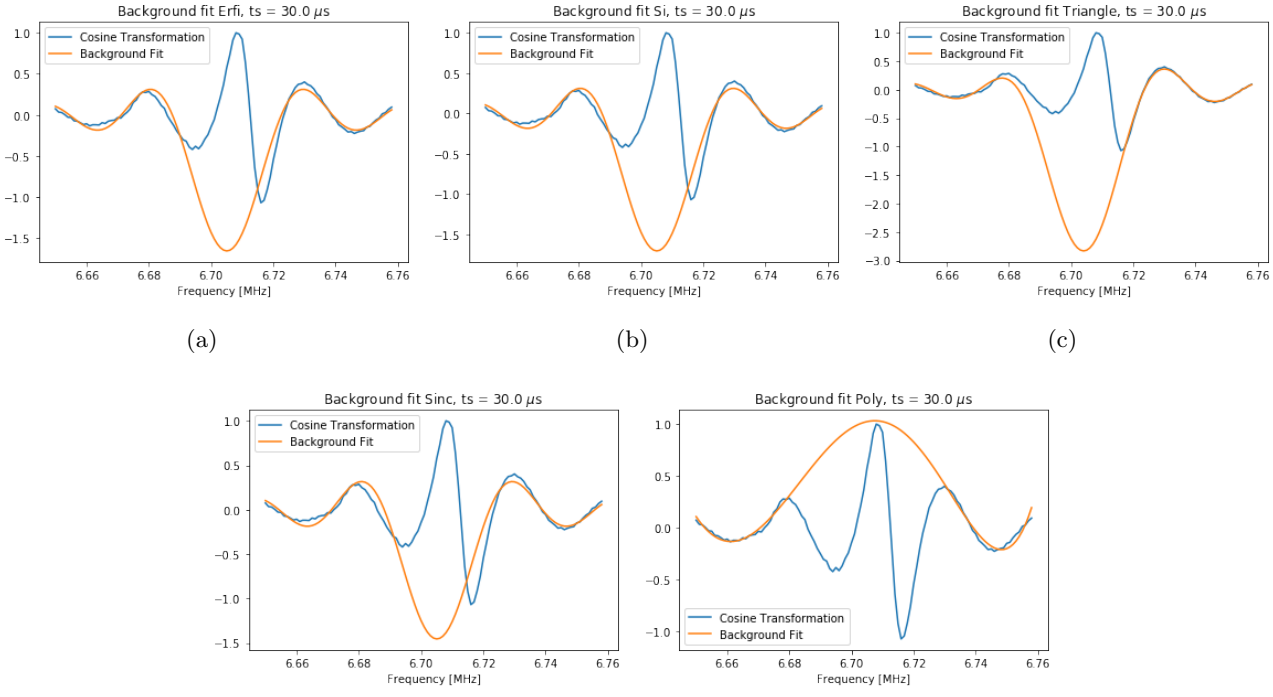


(a) (b) (c)

(d) (e)

Figure 30: Fitting the frequency background 1.5 kHz away from the minima with $t_s = 30$ $\mu$s. The five fit functions are shown: (a) erfi, (b) Si, (c) triangle, (d) sinc, (e) poly.

## 5.2 E-field comparison

We showed in the previous section how the background can be fitted for different start times. In figure 31 we show how the difference in the recovered E-field and the actual E-field corrections change with increasing values of $t_s$.

The polynomial fit can recover the E-field correction up to about 10 $\mu$s before it can no longer be fitted to the background. The sinc fit is valid for about 13 $\mu$s. The erfi and Si fits are valid up to about 23 $\mu$s before they completely break down. The triangular fit we can see has an E-field difference of about 200 ppb by 30 $\mu$s which is due to the large statistical uncertainty of the Monte Carlo simulation for this large value of $t_s$.

This means that all of the fit functions are valid for $t_s$ of up to almost 10 $\mu$s for a realistic Monte Carlo allowing the beam-line positron contamination of the muon beam to be skipped. With higher statistics and using the full Fourier method, the triangular frequency distribution may be fitted to the background all the way up to 30 $\mu$s allowing us to skip scraping entirely. We can confidently recover the frequency distribution for $t_s = 25$ $\mu$s and the effects of scraping is probably negligible between 25 and 30 $\mu$s since there is more scraping in the beginning of the fast rotation signal.

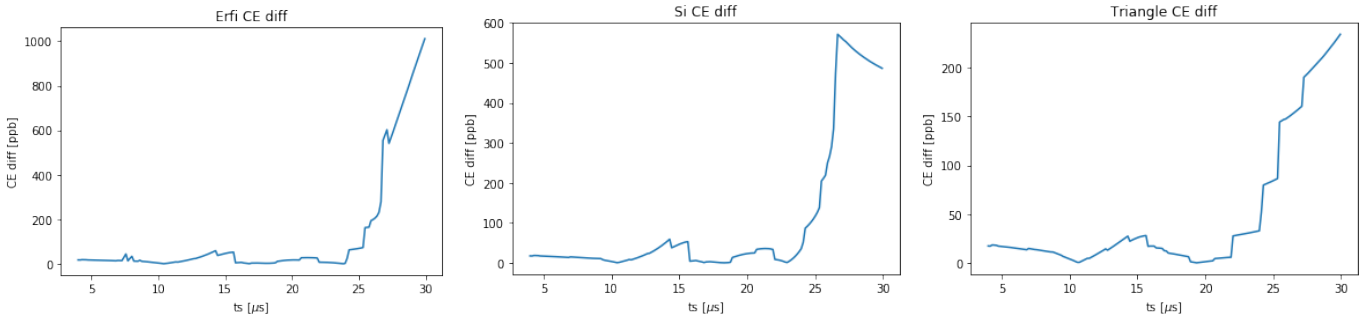


(a) (b) (c)

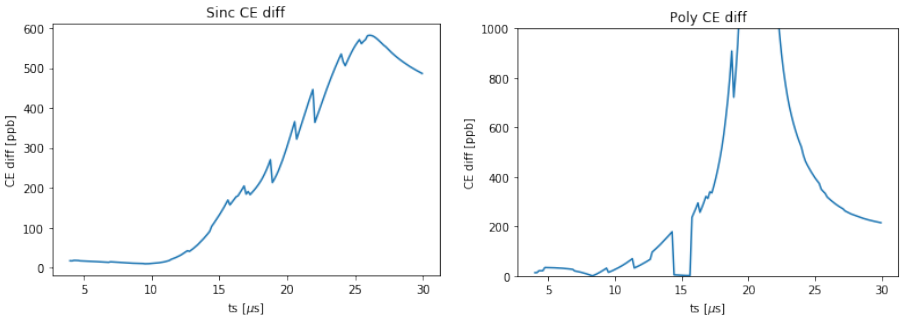


(d) (e)

Figure 31: The difference in the recovered and actual E-field correction vs start time. Five different fit functions are used: (a) erfi, (b) Si, (c) triangle, (d) sinc, (e) poly.

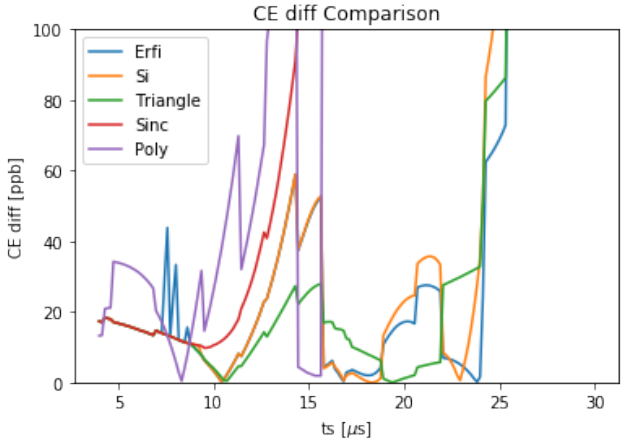


Figure 32: The difference in the recovered and actual E-field correction vs start time with all 5 different fitting functions.

# 6 Conclusion of background fit method

We derived the analytic form of the frequency background for delta function, step function, Gaussian, and triangular frequency distributions, and we used these equations to fit the background and subtract it from the cosine Fourier transformation to obtain the corrected frequency distribution. Using the analytic form of the Gaussian, we were able to correct for the missing time all the way up to $t_s = 30$ $\mu$s for a Monte Carlo fast rotation signal with Gaussian frequency distribution succeeding in the goal of skipping scraping.

When we use a more realistic asymmetric frequency distribution with statistical fluctuations for the Monte Carlo, we were able to use the analytic form of a triangular frequency distribution to fit the background decently all the way up to $t_s = 30$ $\mu$s. At this late start time the frequency distribution cannot be accurately recovered still mostly because of the statistical uncertainty of the Monte Carlo fast rotation signal. We can confidently confidently recover the frequency distributions values of $t_s$ as large as 25 $\mu$s allowing us to skip almost all of scraping since scraping is probably negligible between 25 and 30 $\mu$s.

To see the background being fitted using the full Fourier method [1] including estimations of statistical and systematic uncertainty on real data sets refer to [6],[7],[8],[9], and Monte Carlo data sets [10]. When we use the full Fourier method we are able to fit the background even more accurately.

# 7 Integral approach to the frequency background

We showed in previous sections that the frequency background can removed by fitting for the background and then subtracting it out to obtain the real frequency distribution. An alternative approach to this method is to directly calculate the background by plugging the frequency into equation (2).

## 7.1 Lifting the frequency distribution

This method is what is used by [5]. The dilemma with this approach is that to calculate the background, we must know the complete frequency distribution, and our goal is to find the complete frequency distribution in the first place. We get around this by using an approximate frequency distribution to plug into our background

equation. We take the normalization of the background to be arbitrary, and we also add an additive term to get the following form for the background:

$$\Delta(\omega) = A \int_{\omega^-}^{\omega^+} \tilde{S}(\omega\prime) \frac{\sin[(\omega - \omega\prime)(t_s - t_0)]}{\omega - \omega\prime} d\omega\prime + B, \tag{25}$$

where we optimize the parameters A and B to fit the background. The additive term B will end up being very small and we only include it since it is used in [5]. Since we do not have the real frequency distribution, $\tilde{S}(\omega)$ is an approximate frequency distribution. The approximate frequency distribution is chosen by looking at the two minima of the cosine Fourier transformation which will be located on each side of the maximum of the cosine Fourier transformation. The values which are between the minima are considered to be the signal, so we take the average of the minima's bin contents and then add this to the cosine Fourier transformation in order to lift the distribution up to the x-axis. All points outside the minima are set to 0. This works for small values of $t_s$ when the signal is much larger than the background, however we know that for large values of $t_s$ the signal and background completely merge.

Figure 33 (a) shows the cosine Fourier transform with vertical lines at the minima. The cosine Fourier transformation is lifted up to the x-axis and the frequency bins outside the minima set to zero which is shown in figure 33 (b). The background is calculated numerically using equation (25) with $\tilde{S}(\omega)$ being the approximated frequency distribution shown in (b).

We see in (c) that the background of the cosine Fourier transformation fits our numerically calculated background well for this small value of $t_s$. In (c) the comparison of the recovered and simulated frequency distribution is shown. The two have only a small 3.43 ppb difference. In figure 34 we see that for $t_s = 8$ $\mu$s the integral method no longer matches the background well and we get a E-field difference of 18.89 ppb. We can see in (b) that part of the frequency distribution is in the negative.

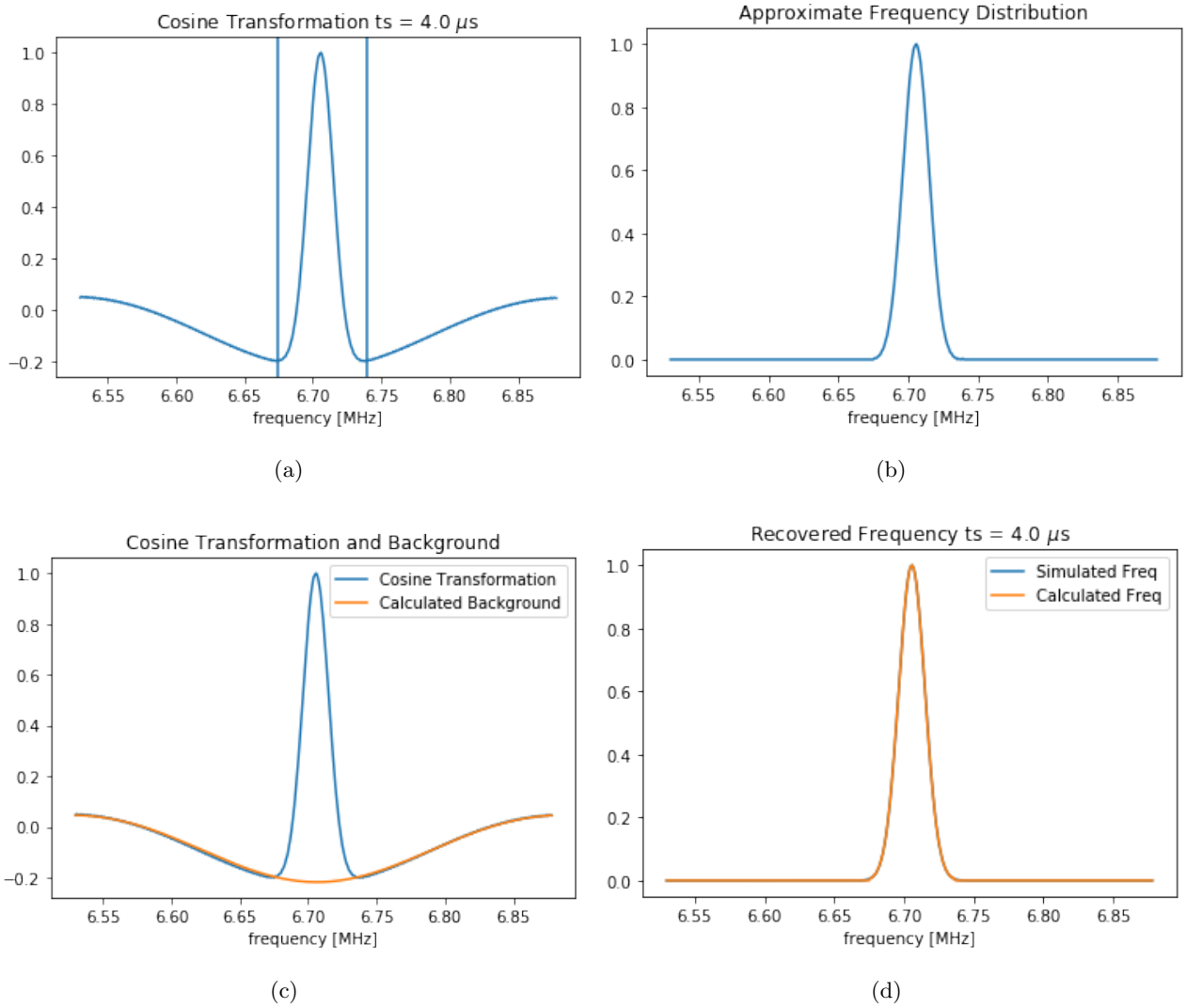


Figure 33: Integral method for $t_s = 4$ $\mu$s. (a) The cosine Fourier transformation of the fast rotation signal with the vertical lines showing the minima, (b) The approximated frequency distribution found by lifting the cosine Fourier transformation, (c) The cosine Fourier transformation with the calculated background, (d) A comparison of the recovered and simulated frequency distributions. A recovered E-field correction of -374.61 ppb and simulated value of -378.04 ppb.

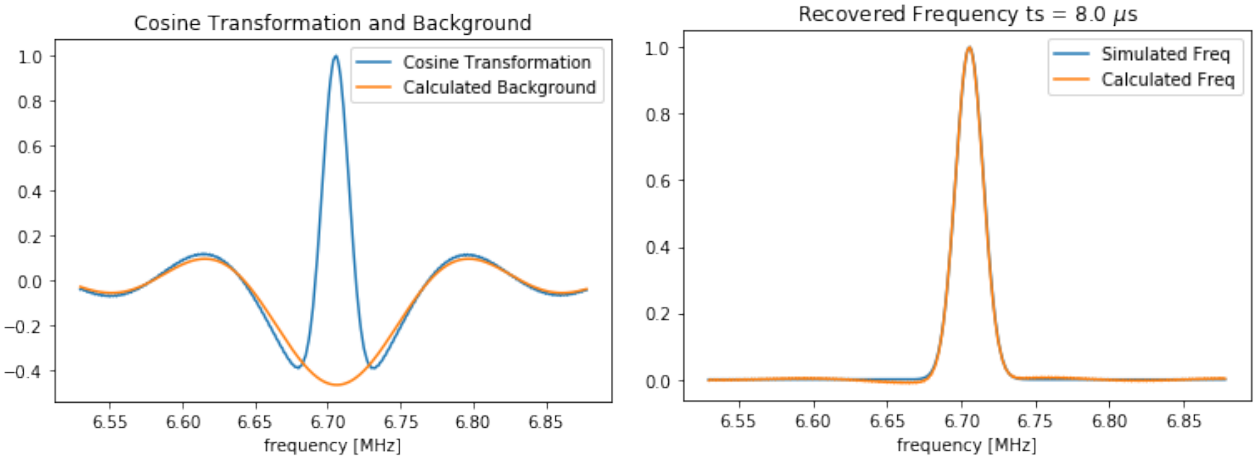


(a) (b)

Figure 34: Integral method for $t_s = 8$ $\mu$s. (a) The cosine Fourier transformation with the calculated background, (b) A comparison of the recovered and simulated frequency distributions. A recovered E-field correction of -350.15 ppb and simulated value of -378.04 ppb.

### 7.2 Iteratively approximating the frequency

In the last section we use an approximate frequency distribution to plug into equation (25) for the background. We can use an iterative process with each iteration using the corrected frequency distribution found in the previous iteration as the approximate frequency distribution to plug into the equation. We always add the correction to the original cosine Fourier transformation, and then use this to as this to calculate the background for the next iteration.

We need to choose $\tilde{S}(\omega)_0$ which is plugged in for the first iteration of the background. We could use the same approximated frequency distribution we used in the last section by lifting the frequency distribution, but the advantage of the iterative approach is that this is not necessary because the background is self corrective. since the background is self corrective it does not matter much what distribution you start with. Here we start by plugging in the actual cosine Fourier transformation in for $\tilde{S}(\omega)_0$, and we still recover the frequency distribution. We then define the iterative definition of the corrected frequency distribution by:

$$\tilde{S}(\omega)_{i+1} = \tilde{S}(\omega)_0 + A_i \int_{\omega^-}^{\omega^+} \tilde{S}(\omega\prime)_i \frac{\sin[(\omega - \omega\prime)(t_s - t_0)]}{\omega - \omega\prime} d\omega\prime + B_i, \tag{26}$$

where the constants A and B are optimized for each iteration. In figure 35 we show the first two iterations for calculating the background. For just one iteration when we use the cosine Fourier transformation as the approximate frequency distribution to calculate the background, we get a recovered $C_E$ = -384.03 ppb compared to the actual $C_E$ = -378.04 ppb which is 5.99 ppb apart. For iteration two we get a recovered $C_E$ = -379.22 ppb which is only 1.18 ppb away from the actual $C_E$. For small values of $t_s$ the iterative process converges after only 3 iterations. This can be seen in figure 36 where we show the difference in $C_E$ between the recovered and actual frequency distributions. After only 3 iterations the $C_E$ difference is flat as the frequency distribution converges to a value.

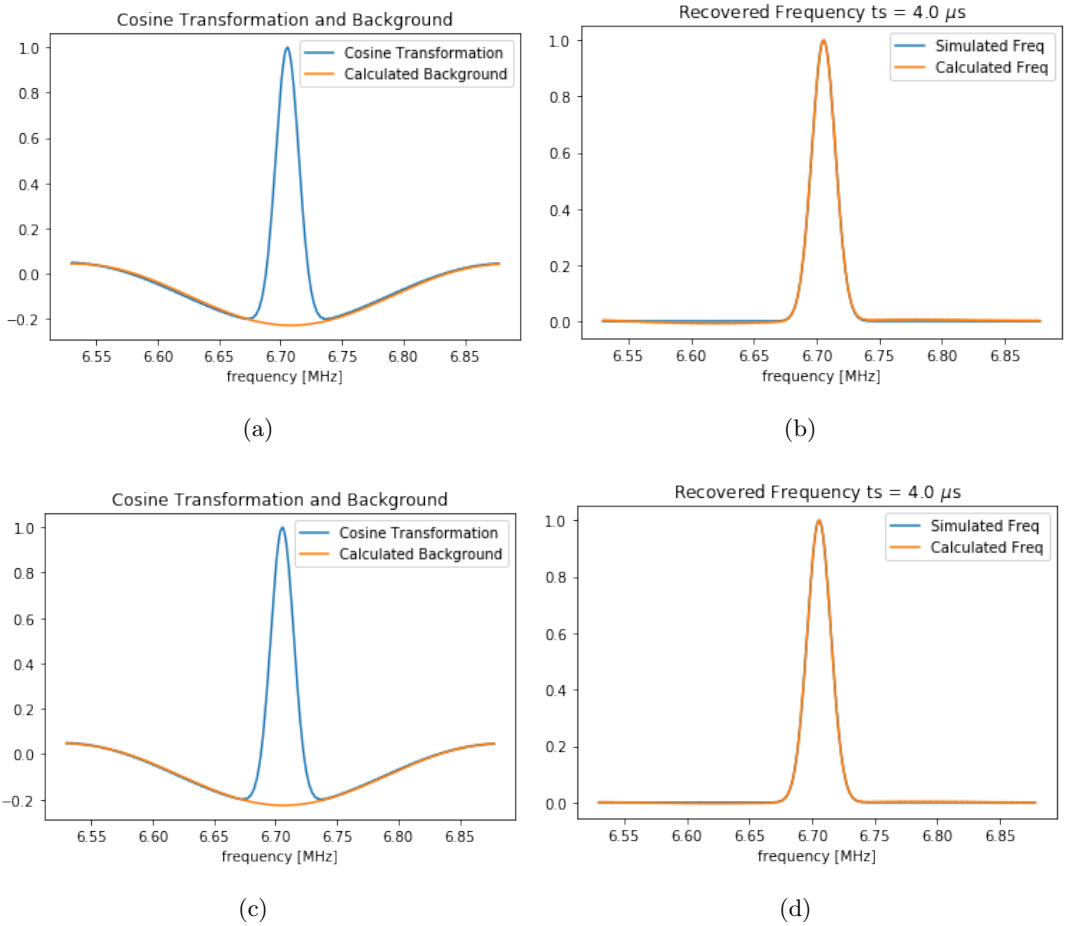


Figure 35: Iterative integral method for $t_s = 4$ $\mu$s. We start with the cosine Fourier transformation as an approximate frequency distribution to find the background. Then each iteration is used as the next approximate frequency distribution for calculating the background. (a) The cosine Fourier transformation and the calculated background for iteration 1, (b) A comparison of the recovered and simulated frequency distributions for iteration 1, (c) The cosine Fourier transformation and the calculated background for iteration 2, (d) A comparison of the recovered and simulated frequency distributions for iteration 2.

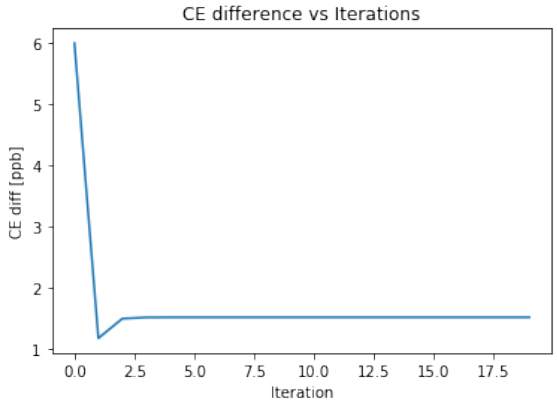


Figure 36: This is the difference between the actual and recovered E-field correction for each iteration using the iterative integral method with $t_s = 4$ $\mu$s. The $C_E$ difference flattens after only a couple of iterations showing the convergence of the frequency distribution.

For larger values of $t_s$ we need more iterations to get an accurate background. Fgure 37 shows the cosine Fourier transformation and the calculated background for the first 4 iterations of the background calculation. For large values of $t_s$, the first two iterations of the background do not match the background much at all, but by the fourth iteration our calculated background has begun to converge close to the actual background of the cosine Fourier transformation. In figure 38 the background is shown after 100 iterations, and the calculated background is very close to the cosine Fourier transformation background. There is no disadvantage to using more iterations so 100 iterations are used even though the background converged long before 100 iterations.

Despite our fit looking decent, the frequency distribution is not exactly recovered since it is slightly lopsided. We get a recovered $C_E$ = -341.98 ppb which is 36.06 ppb away from the actual E-field correction. If we compare the background we get in figure 38 (a) to the background obtained in figure 34 (a) we see that the background for the iterative method is much closer to the cosine Fourier transformation, although the recovered frequency distributions are similarly off. In figure 39 we show how the $C_E$ difference does not change after just 5 iterations.

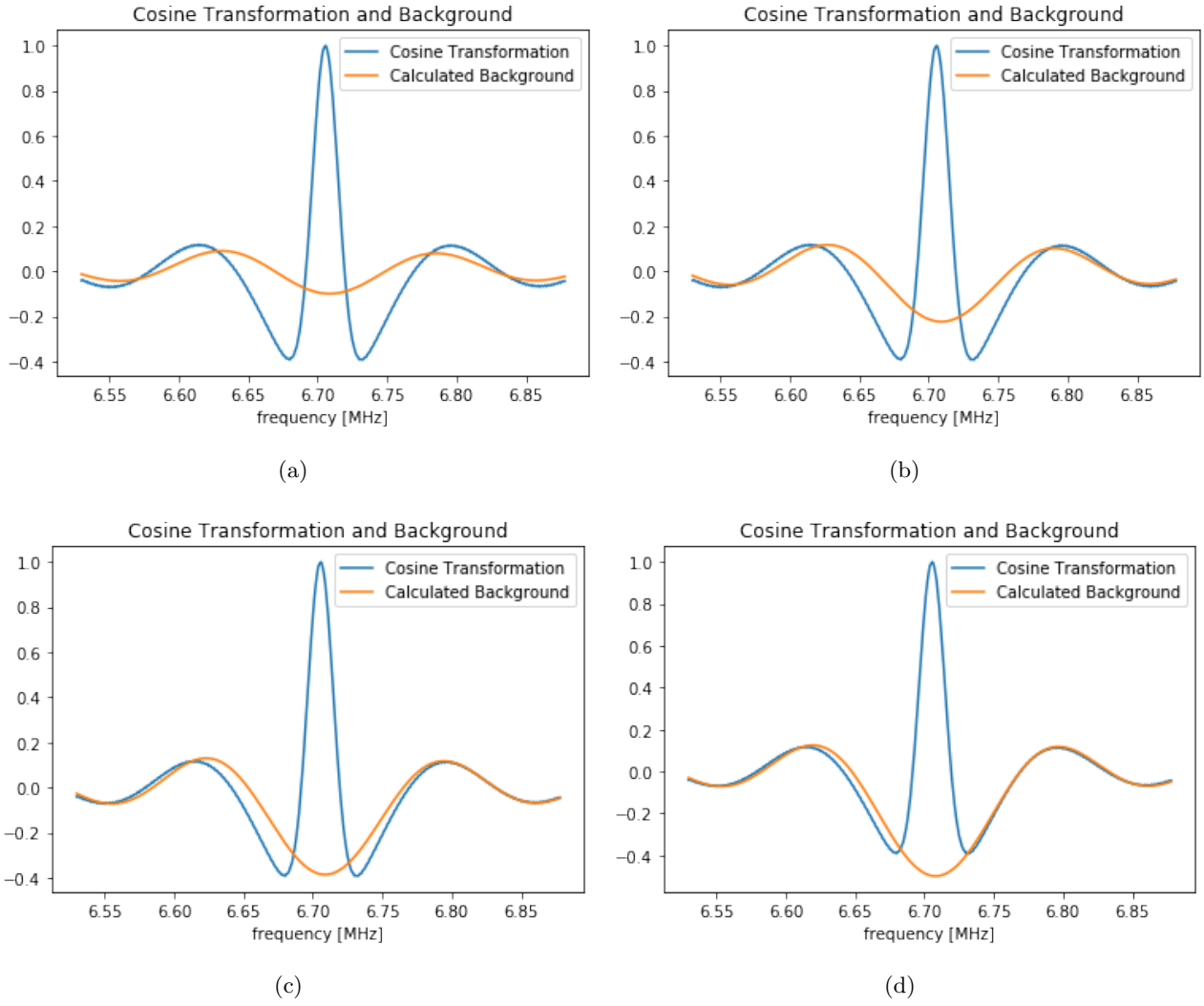


Figure 37: This is the cosine Fourier transformation and the calculated background for the iterative integral method with $t_s = 8$ $\mu$s. Four iterations are shown: (a) Iteration 1, (b) Iteration 2, (c) Iteration 3, (d) Iteration 4.

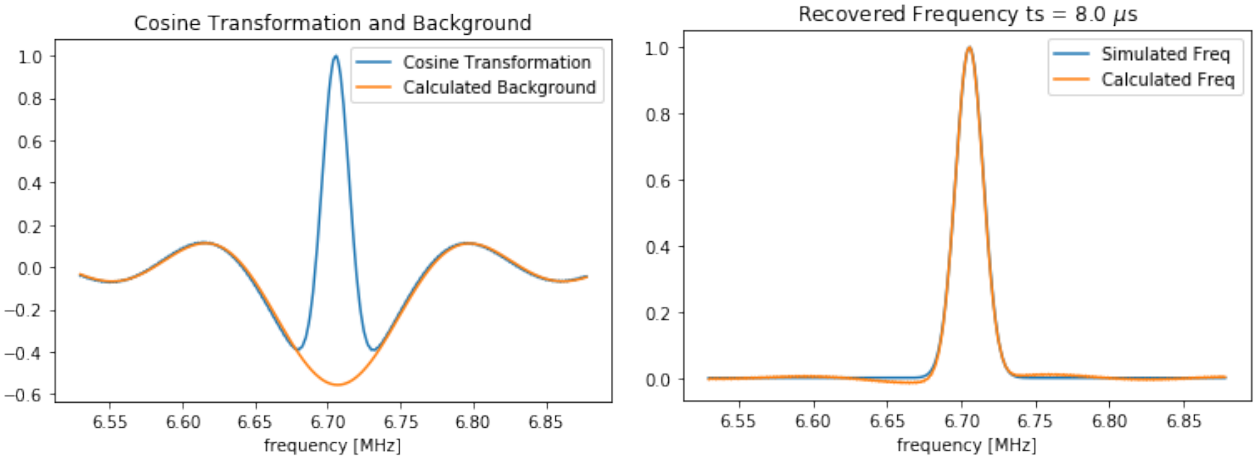


(a) (b)

Figure 38: This is the cosine Fourier transformation and the calculated background for the iterative integral method with $t_s = 8$ $\mu$s after 100 iterations. (a) The cosine Fourier transformation and the calculated background, (b) A comparison of the recovered and simulated frequency distributions.

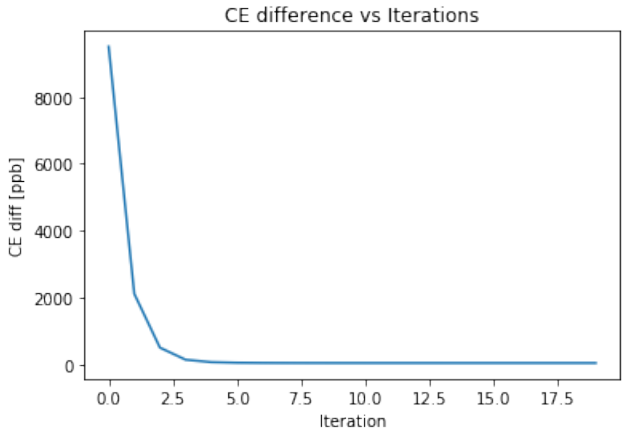


Figure 39: This is the difference between the actual and recovered E-field correction for each iteration using the iterative integral method with $t_s = 8$ $\mu$s.

## 8 Conclusion of integration method

The integral approach is not as effective as fitting the background to the cosine Fourier transformation since it relies on knowledge of the frequency distribution. The goal when fitting for the background is to use a general enough analytic form so that the background can be fitted regardless of the form of the frequency distribution. The integral method is not as general since we have to figure out the form of the frequency distribution in order to make the correction.

We could improve this method by using the recover the frequency distribution for $t_s = 4$ $\mu$s ,and then use this as the approximate frequency distribution for higher values of $t_s$. The iterative approach would still fail, however for large values of $t_s$.

It is possible the integral method could be developed to a point where it can compete with the fit method,

but as it currently stands it cannot be used to skip scraping. The integral method can still be useful however since it can use this method in conjunction with the fit method for $t_s = 4$ $\mu$s as a way of checking that the background is properly eliminated for real data when we the real frequency distribution is unknown, and then use difference in the recovered E-field correction between the two methods can be considered a systematic uncertainty of the Fourier method.

# Appendices

## A When is $t_s$ small?

We consider $t_s$ to be small when we can Taylor expand the sin function in (3). This is possible when $|(t_s - t_0)(\omega - \omega\prime)| \ll 1$. The $\omega - \omega\prime$ is only relevant where the frequency distribution $\tilde{S}(\omega)$ is non-zero so this is approximately when the frequency is within a few standard deviations from the frequency distribution. If we assume that the full 5 standard deviation frequency distribution is confined within the collimator aperture, then $t_s$ is small when $5(t_s - t_0)\sigma \ll 1$. Values of $t_0$ are much smaller than $t_s$ since $t_0$ is between 0 and 150 ns while $t_s$ will be at least 4 $\mu$s, so we define $t_s$ to be small explicitly when $5t_s\sigma \ll 1$. This makes it so that we the background can be fitted for higher values of $t_s$ when the frequency distribution has smaller width.

For small enough values of $t_s$, the background is approximately a parabola. We can see this in figure 40 where we show the background for a Gaussian frequency distribution for a value of $t_s = 4$ $\mu$s. We show explicitly in section 4.1 that the we can Taylor expand the background itself for small values of $t_s$. Other forms of the frequency background require less approximations to be made so we can use much higher values of $t_s$ than 4 $\mu$s.

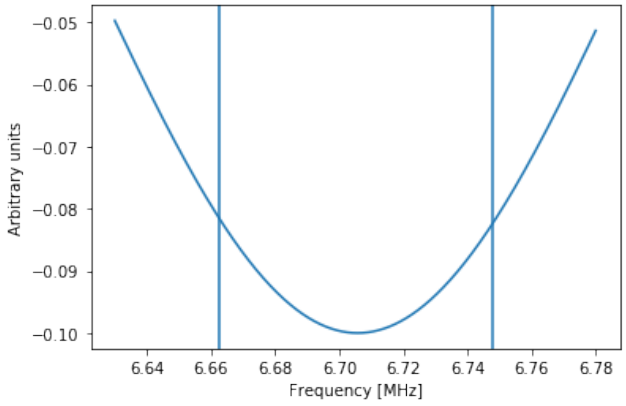


Figure 40: Frequency background from a Gaussian frequency distribution with $t_0 = 0$ $\mu$s and $t_s = 4$ $\mu$s. The vertical lines are the bounds of the collimator aperture. For this small value of $t_s$ the background is approximately parabolic.

## B Approximating the step function to be a Gaussian

We want to show that we can use the form of the background distribution which we found in section 2.3 and 2.2 when the frequency distribution is Gaussian or skewed Gaussian. This also includes the triangular frequency distribution because if the step function background can be used to approximate the Gaussian background then the triangular background can certainly do it too. This justifies what was shown visually in figure 7 that the

Gaussian, step function, and triangular frequency distributions all produce approximately the same background for small values of $t_s$.

### B.1 Gaussian frequency distribution

We start by Taylor expanding the Gaussian frequency distribution and plug into the equation for the correction of the cosine Fourier transformation to show that in the limit when $t_s$ is small the Gaussian frequency is has the same form as the step function:

$$\tilde{S}(\omega) = \frac{1}{\sqrt{2\pi\sigma^2}}(1 - \frac{(\omega-\omega_0)^2}{2\sigma^2} + \frac{(\omega-\omega_0)^4}{8\sigma^4} + ...). \tag{27}$$

Then we can plug in the Taylor expanded series into our equation for $\Delta(\omega)$:

$$\begin{aligned}\Delta(\omega) &= \frac{1}{\pi}\int_{\omega^-}^{\omega^+} \frac{1}{\sqrt{2\pi\sigma^2}}(1 - \frac{(\omega\prime-\omega_0)^2}{2\sigma^2} + \frac{(\omega\prime-\omega_0)^4}{8\sigma^4} + ...)\frac{\sin[(\omega-\omega\prime)(t_s-t_0)]}{\omega-\omega\prime}d\omega\prime \\ &= \frac{1}{\sqrt{2\pi^3\sigma^2}}\int_{\omega^-}^{\omega^+}(1 - \frac{(\omega\prime-\omega_0)^2}{2\sigma^2} + \frac{(\omega\prime-\omega_0)^4}{8\sigma^4} + ...)\frac{\sin[(\omega-\omega\prime)(t_s-t_0)]}{\omega-\omega\prime}d\omega\prime.\end{aligned} \tag{28}$$

When we integrate these first terms we get:

$$\begin{aligned}\Delta(\omega) = \frac{1}{\sqrt{2\pi^3\sigma^2}}\Big[&\mathrm{Si}((\omega-\omega^-)(t_s-t_0)) - \mathrm{Si}((\omega-\omega^+)(t_s-t_0)) \\ &+ \frac{(\omega-\omega_0)^2}{2\sigma^2}Si((\omega-\omega^-)(t_s-t_0)) - \mathrm{Si}((\omega-\omega^+)(t_s-t_0)) \\ &+ \frac{\sin[(\omega-\omega^-)(t_s-t_0)] + (t_s-t_0)(\omega+\omega^- - 2\omega_0)\cos[(\omega-\omega^-)(t_s-t_0)]}{2\sigma^2(t_s-t_0)^2} - \frac{\sin[(\omega-\omega^+)(t_s-t_0)] + (t_s-t_0)(\omega+\omega^+ - 2\omega_0)\cos[(\omega-\omega^+)(t_s-t_0)]}{2\sigma^2(t_s-t_0)^2} \\ &+ \frac{(\omega-\omega_0)^4}{8\sigma^4}Si((\omega-\omega^-)(t_s-t_0)) - \mathrm{Si}((\omega-\omega^+)(t_s-t_0) \\ &+ \frac{\big((t_s-t_0)^2[(6\omega_0^2 - 4\omega_0(\omega+2\omega^-) + (\omega^2+2\omega^-\omega+3\omega_-^2)] - 6\big)\sin[(\omega-\omega^-)(t_s-t_0)]}{8\sigma^4(t_s-t_0)^4} \\ &- \frac{\big((t_s-t_0)^2[(6\omega_0^2 - 4\omega_0(\omega+2\omega^+) + (\omega^2+2\omega^+\omega+3\omega_+^2)] - 6\big)\sin[(\omega-\omega^+)(t_s-t_0)]}{8\sigma^4(t_s-t_0)^4} \\ &+ \frac{(t_s-t_0)[(t_s-t_0)^2\big[-4\omega_0^3 + 6\omega_0(\omega+\omega^-) - 4\omega_0(\omega^2+\omega^-\omega+\omega_-^2) + \omega^3+\omega^-\omega^2+\omega_-^2\omega+\omega_-^3\big] - 2\omega - \omega^- + 8\omega_0]\cos[(\omega-\omega^-)(t_s-t_0)]}{8\sigma^4(t_s-t_0)^4} \\ &- \frac{(t_s-t_0)[(t_s-t_0)^2\big[-4\omega_0^3 + 6\omega_0(\omega+\omega^+) - 4\omega_0(\omega^2+\omega^+\omega+\omega_+^2) + \omega^3+\omega^+\omega^2+\omega_+^2\omega+\omega_+^3\big] - 2\omega - \omega^+ + 8\omega_0]\cos[(\omega-\omega^+)(t_s-t_0)]}{8\sigma^4(t_s-t_0)^4} + ...\Big].\end{aligned} \tag{29}$$

This looks like a complicated equation for the correction, but we can make some approximations to show that the complicated sine and cosine terms are small compared to the Si terms. If we just look at the second term in the expansion:

$$\Delta(\omega)_2 = \int_{\omega^-}^{\omega^+} \frac{(\omega\prime - \omega_0)^2}{2\sigma^2} \frac{\sin[(\omega - \omega\prime)(t_s - t_0)]}{\omega - \omega\prime} d\omega\prime =$$
$$\frac{1}{2\sigma^2}\big[(\omega - \omega_0)^2[\mathrm{Si}((\omega - \omega^-)(t_s - t_0)) - \mathrm{Si}((\omega - \omega^+)(t_s - t_0))]$$
$$+ \frac{\sin[(\omega - \omega^-)(t_s - t_0)] + (t_s - t_0)(\omega + \omega^- - 2\omega_0)\cos[(\omega - \omega^-)(t_s - t_0)]}{(t_s - t_0)^2}$$
$$- \frac{\sin[(\omega - \omega^+)(t_s - t_0)] + (t_s - t_0)(\omega + \omega^+ - 2\omega_0)\cos[(\omega - \omega^+)(t_s - t_0)]}{(t_s - t_0)^2}\big]. \tag{30}$$

We make the assumption that $|(\omega - \omega^-)(t_s - t_0)|$ and $|(\omega - \omega^+)(t_s - t_0)|$ are small quantities such that we can invoke the small angle approximation $\sin(x) \approx x$ and $\cos(x) \approx 1$ for $|x| \ll 1$. Then we can say that $\sin[(\omega - \omega^-)(t_s - t_0)] \approx (\omega - \omega^-)(t_s - t_0)$, $\sin[(\omega - \omega^+)(t_s - t_0)] \approx (\omega - \omega^+)(t_s - t_0)$ and $\cos[(\omega - \omega^-)(t_s - t_0)] \approx 1$, $\cos[(\omega - \omega^+)(t_s - t_0)] \approx 1$. When we make this assumption in for $\Delta(\omega)_2$, the second term in the background Taylor expansion, we get the following cancellation:

$$\Delta(\omega)_2 = \int_{\omega^-}^{\omega^+} \frac{(\omega\prime - \omega_0)^2}{2\sigma^2} \frac{\sin[(\omega - \omega\prime)(t_s - t_0)]}{\omega - \omega\prime} d\omega\prime \approx$$
$$\frac{1}{2\sigma^2}\big[(\omega - \omega_0)^2[\mathrm{Si}((\omega - \omega^-)(t_s - t_0)) - \mathrm{Si}((\omega - \omega^+)(t_s - t_0))]$$
$$+ \frac{(\omega - \omega^-)(t_s - t_0) + (t_s - t_0)(\omega + \omega^- - 2\omega_0)}{(t_s - t_0)^2} - \frac{(\omega - \omega^+)(t_s - t_0) + (t_s - t_0)(\omega + \omega^+ - 2\omega_0)}{(t_s - t_0)^2}\big]$$
$$= \frac{1}{2\sigma^2}\big[(\omega - \omega_0)^2[\mathrm{Si}((\omega - \omega^-)(t_s - t_0)) - \mathrm{Si}((\omega - \omega^+)(t_s - t_0))]$$
$$+ \frac{[(\omega - \omega^-) + (\omega + \omega^- - 2\omega_0)] - [(\omega - \omega^+) + (\omega + \omega^+ - 2\omega_0)]}{(t_s - t_0)}\big]$$
$$= \frac{1}{2\sigma^2}\big[(\omega - \omega_0)^2[\mathrm{Si}((\omega - \omega^-)(t_s - t_0)) - \mathrm{Si}((\omega - \omega^+)(t_s - t_0))] + \frac{2(\omega - \omega_0) - 2(\omega - \omega_0)}{(t_s - t_0)}\big]$$
$$= \frac{(\omega - \omega_0)^2}{2\sigma^2}[\mathrm{Si}((\omega - \omega^-)(t_s - t_0)) - \mathrm{Si}((\omega - \omega^+)(t_s - t_0)), \tag{31}$$

so the sine and cosine terms have been eliminated. We also want to make sure that the Si terms do not cancel like the sine and cosine terms do under the small angle approximation. The Si function has a Taylor expansion like where $\mathrm{Si}(x) = x - x^3/18 + x^5/600 + ...$ , and we can then make the approximation that $\mathrm{Si}(x) \approx x$ for $|x| \ll 1$.

We can check now that under this approximation the Si terms does not cancel:

$$\Delta(\omega)_2 = \int_{\omega^-}^{\omega^+} \frac{(\omega\prime - \omega_0)^2}{2\sigma^2} \frac{\sin[(\omega - \omega\prime)(t_s - t_0)]}{\omega - \omega\prime} d\omega\prime \approx \frac{(\omega - \omega_0)^2}{2\sigma^2} [\mathrm{Si}((\omega - \omega^-)(t_s - t_0)) - \mathrm{Si}((\omega - \omega^+)(t_s - t_0))$$
$$\approx \frac{(\omega - \omega_0)^2}{2\sigma^2} [(\omega - \omega^-)(t_s - t_0) - (\omega - \omega^+)(t_s - t_0)]$$
$$= \frac{(t_s - t_0)(\omega^+ - \omega^-)(\omega - \omega_0)^2}{2\sigma^2}. \tag{32}$$

This term has nontrivial $\omega$ dependence in the approximation so the Si terms cannot be left out. So in the small angle approximation we eliminate the sine and cosine terms but leave the Si function so that:

$$\Delta(\omega) \approx \frac{1}{\sqrt{2\pi^3\sigma^2}} \big[ \mathrm{Si}((\omega - \omega^-)(t_s - t_0)) - \mathrm{Si}((\omega - \omega^+)(t_s - t_0))$$
$$+ \frac{(\omega - \omega_0)^2}{2\sigma^2} Si((\omega - \omega^-)(t_s - t_0)) - \mathrm{Si}((\omega - \omega^+)(t_s - t_0))$$
$$+ \frac{(\omega - \omega_0)^4}{8\sigma^4} Si((\omega - \omega^-)(t_s - t_0)) - \mathrm{Si}((\omega - \omega^+)(t_s - t_0) + ...\big]. \tag{33}$$

When we group the Si terms together we get:

$$\Delta(\omega) = \frac{1}{\sqrt{2\pi^3\sigma^2}} (1 - \frac{(\omega - \omega_0)^2}{2\sigma^2} + \frac{(\omega - \omega_0)^4}{8\sigma^4} + ...) \big[ \mathrm{Si}((\omega - \omega^-)(t_s - t_0)) - \mathrm{Si}((\omega - \omega^+)(t_s - t_0)) \big], \tag{34}$$

and we have recovered the Taylor series for the Gaussian so we can restore our original signal:

$$\Delta(\omega) = \frac{1}{\sqrt{2\pi^3\sigma^2}} e^{-\frac{(\omega\prime - \omega_0)^2}{2\sigma^2}} \big[ \mathrm{Si}((\omega - \omega^-)(t_s - t_0)) - \mathrm{Si}((\omega - \omega^+)(t_s - t_0)) \big]. \tag{35}$$

We have shown that for a frequency distribution $\tilde{S}(\omega)$ which is Gaussian, we the correction take the following approximate form:

$$\Delta(\omega) = \frac{1}{\pi} \int_{\omega^-}^{\omega^+} \tilde{S}(\omega\prime) \frac{\sin[(\omega - \omega\prime)(t_s - t_0)]}{\omega - \omega\prime} d\omega\prime \approx \frac{1}{\pi} \tilde{S}(\omega) \big[ \mathrm{Si}((\omega - \omega^-)(t_s - t_0)) - \mathrm{Si}((\omega - \omega^+)(t_s - t_0)) \big]. \tag{36}$$

This is the same form as when we used a step function as our frequency distribution, since if we plugged in the step function in equation 7 in for $\tilde{S}(\omega)$ then we would recover the exact equation (22) for the frequency background found using the step function. This means we can use the step function approximation of the frequency distribution to fit the frequency background even for the Gaussian frequency distribution.

### B.2 Skewed Gaussian frequency distribution

We can now try using a skewed Gaussian so that we do not have an even frequency distribution If we assume a skewed Gaussian frequency distribution centered at the magic frequency $\omega_0$ with a standard deviation $\sigma$ and now we define the skew of the Gaussian as $\alpha$:

$$\tilde{S}(\omega) = \frac{1}{\sqrt{2\pi\sigma^2}} e^{-\frac{(\omega-\omega_0)^2}{2\sigma^2}} [1 + \text{erf}(\frac{\alpha(\omega-\omega_0)}{\sqrt{2}\sigma})]. \tag{37}$$

Then we plug into the equation for the correction to the cosine Fourier transformation:

$$\Delta(\omega) = \frac{1}{\pi}\int_{\omega^-}^{\omega^+} \tilde{S}(\omega\prime)\frac{\sin[(\omega-\omega\prime)(t_s-t_0)]}{\omega-\omega\prime}d\omega\prime = \frac{1}{\sqrt{2\pi^3\sigma^2}}\int_{\omega^-}^{\omega^+} e^{-\frac{(\omega\prime-\omega_0)^2}{2\sigma^2}}[1+\text{erf}(\frac{\alpha(\omega\prime-\omega_0)}{\sqrt{2}\sigma})]\frac{\sin[(\omega-\omega\prime)(t_s-t_0)]}{\omega-\omega\prime}d\omega\prime$$
$$= \frac{1}{\sqrt{2\pi^3\sigma^2}}\big[\int_{\omega^-}^{\omega^+} e^{-\frac{(\omega\prime-\omega_0)^2}{2\sigma^2}}\frac{\sin[(\omega-\omega\prime)(t_s-t_0)]}{\omega-\omega\prime}d\omega\prime + \int_{\omega^-}^{\omega^+} e^{-\frac{(\omega\prime-\omega_0)^2}{2\sigma^2}}\,\text{erf}(\frac{\alpha(\omega\prime-\omega_0)}{\sqrt{2}\sigma})\frac{\sin[(\omega-\omega\prime)(t_s-t_0)]}{\omega-\omega\prime}d\omega\prime\big]. \tag{38}$$

The first term we get is exactly the same term we solved for in the case of the Gaussian frequency distribution with our earlier approximation so we already know the answer to that and can plug in:

$$\Delta(\omega) \approx \frac{1}{\sqrt{2\pi^3\sigma^2}}\big[e^{-\frac{(\omega\prime-\omega_0)^2}{2\sigma^2}}\big[\,\text{Si}((\omega-\omega^-)(t_s-t_0)) - \text{Si}((\omega-\omega^+)(t_s-t_0))\big]$$
$$+\int_{\omega^-}^{\omega^+} e^{-\frac{(\omega\prime-\omega_0)^2}{2\sigma^2}}\,\text{erf}(\frac{\alpha(\omega\prime-\omega_0)}{\sqrt{2}\sigma})\frac{\sin[(\omega-\omega\prime)(t_s-t_0)]}{\omega-\omega\prime}d\omega\prime\big] \tag{39}$$

We can try and figure out what the second term by assuming that the erf function is small. The Taylor expansion of the erf function is as follows:

$$\text{erf}(x) = \frac{2}{\sqrt{\pi}}\sum_{n=0}^{\infty}\frac{(-1)^n x^{2n+1}}{n!(2n+1)} = \frac{2}{\sqrt{\pi}}\big(x - \frac{x^3}{3} + \frac{x^5}{10} - \frac{x^7}{42} + ...\big), \tag{40}$$

and since $\omega\prime$ is bounded $\omega^- \leq \omega\prime \leq \omega^+$, we can say that the argument of the erf function $\frac{\alpha(\omega\prime-\omega_0)}{\sqrt{2}\sigma}$ is small for small $\alpha$. Therefore, when $\frac{(\omega\prime-\omega_0)}{\sigma} \sim 1$ and $|\alpha| \ll 1$ we can make the approximation that:

$$\text{erf}[\frac{\alpha(\omega\prime-\omega_0)}{\sqrt{2}\sigma}] \approx \sqrt{\frac{2}{\pi}}\frac{\alpha(\omega\prime-\omega_0)}{\sigma}. \tag{41}$$

In this small skewness limit, we can plug this approximation into the equation for the correction:

$$\Delta(\omega) \approx \frac{1}{\sqrt{2\pi^3\sigma^2}}\Bigg[e^{-\frac{(\omega\prime-\omega_0)^2}{2\sigma^2}}\big[\,\text{Si}((\omega-\omega^-)(t_s-t_0)) - \text{Si}((\omega-\omega^+)(t_s-t_0))\big]$$
$$+\int_{\omega^-}^{\omega^+} e^{-\frac{(\omega\prime-\omega_0)^2}{2\sigma^2}}\sqrt{\frac{2}{\pi}}\frac{\alpha(\omega\prime-\omega_0)}{\sigma}\frac{\sin[(\omega-\omega\prime)(t_s-t_0)]}{\omega-\omega\prime}d\omega\prime\Bigg]$$
$$\approx \frac{1}{\sqrt{2\pi^3\sigma^2}}e^{-\frac{(\omega\prime-\omega_0)^2}{2\sigma^2}}\big[\,\text{Si}((\omega-\omega^-)(t_s-t_0)) - \text{Si}((\omega-\omega^+)(t_s-t_0))\big]$$
$$+\frac{\alpha}{\pi^2\sigma^2}\int_{\omega^-}^{\omega^+} e^{-\frac{(\omega\prime-\omega_0)^2}{2\sigma^2}}(\omega\prime-\omega_0)\frac{\sin[(\omega-\omega\prime)(t_s-t_0)]}{\omega-\omega\prime}d\omega\prime. \tag{42}$$

We can then Taylor expand the Gaussian as we did before for the case of a Gaussian frequency distribution:

$$\Delta(\omega) \approx \frac{1}{\sqrt{2\pi^3\sigma^2}} e^{-\frac{(\omega\prime-\omega_0)^2}{2\sigma^2}} \big[\,\mathrm{Si}((\omega-\omega^-)(t_s-t_0)) - \mathrm{Si}((\omega-\omega^+)(t_s-t_0))\big]$$

$$+ \frac{\alpha}{\pi^2\sigma^2}\int_{\omega^-}^{\omega^+} e^{-\frac{(\omega\prime-\omega_0)^2}{2\sigma^2}}(\omega\prime-\omega_0)\frac{\sin[(\omega-\omega\prime)(t_s-t_0)]}{\omega-\omega\prime}d\omega\prime$$

$$= \frac{1}{\sqrt{2\pi^3\sigma^2}} e^{-\frac{(\omega\prime-\omega_0)^2}{2\sigma^2}} \big[\,\mathrm{Si}((\omega-\omega^-)(t_s-t_0)) - \mathrm{Si}((\omega-\omega^+)(t_s-t_0))\big]$$

$$+ \frac{\alpha}{\pi^2\sigma^2}\int_{\omega^-}^{\omega^+} (1 - \frac{(\omega\prime-\omega_0)^2}{2\sigma^2} + \frac{(\omega\prime-\omega_0)^4}{8\sigma^4} + ...)(\omega\prime-\omega_0)\frac{\sin[(\omega-\omega\prime)(t_s-t_0)]}{\omega-\omega\prime}d\omega\prime$$

$$= \frac{1}{\sqrt{2\pi^3\sigma^2}} e^{-\frac{(\omega\prime-\omega_0)^2}{2\sigma^2}} \big[\,\mathrm{Si}((\omega-\omega^-)(t_s-t_0)) - \mathrm{Si}((\omega-\omega^+)(t_s-t_0))\big]$$

$$+ \frac{\alpha}{\pi^2\sigma^2}\int_{\omega^-}^{\omega^+} [(\omega\prime-\omega_0) - \frac{(\omega\prime-\omega_0)^3}{2\sigma^2} + \frac{(\omega\prime-\omega_0)^5}{8\sigma^4} + ...]\frac{\sin[(\omega-\omega\prime)(t_s-t_0)]}{\omega-\omega\prime}d\omega\prime$$

$$= \frac{1}{\sqrt{2\pi^3\sigma^2}} \big[e^{-\frac{(\omega\prime-\omega_0)^2}{2\sigma^2}} \big[\,\mathrm{Si}((\omega-\omega^-)(t_s-t_0)) - \mathrm{Si}((\omega-\omega^+)(t_s-t_0))\big]$$

$$+ \frac{\alpha}{\pi^2\sigma^2}\Bigg[(\omega-\omega_0)[\mathrm{Si}((\omega-\omega^-)(t_s-t_0)) - \mathrm{Si}((\omega-\omega^+)(t_s-t_0)] + \frac{\cos[(\omega-\omega^-)(t_s-t_0)] - \cos[(\omega-\omega^+)(t_s-t_0)]}{(t_s-t_0)}$$

$$+ \frac{1}{2\sigma^2}\Bigg[(\omega-\omega_0)^3[\mathrm{Si}((\omega-\omega^-)(t_s-t_0)) - \mathrm{Si}((\omega-\omega^+)(t_s-t_0)]$$

$$+ \frac{(\omega+2\omega^- - 3\omega_0)\sin[(\omega-\omega^-)(t_s-t_0)]}{(t_s-t_0)^2} - \frac{(\omega+2\omega^+ - 3\omega_0)\sin[(\omega-\omega^+)(t_s-t_0)]}{(t_s-t_0)^2}$$

$$+ \frac{((t_s-t_0)^2[3\omega_0^2 - 3\omega_0(\omega^-+\omega) + (\omega_-^2 + \omega^-\omega + \omega^2)] - 2)\cos[(\omega-\omega^-)(t_s-t_0)]}{(t_s-t_0)^3}$$

$$- \frac{((t_s-t_0)^2[3\omega_0^2 - 3\omega_0(\omega^++\omega) + (\omega_+^2 + \omega^+\omega + \omega^2)] - 2)\cos[(\omega-\omega^+)(t_s-t_0)]}{(t_s-t_0)^3} + ...\Bigg]. \quad (43)$$

This equation for the correction looks complicated, but we can simplify the sine and cosine terms just like we did for the case of a Gaussian frequency distribution. We do this by making the assumption that $|(\omega-\omega^+)(t_s-t_0)| \ll 1$ and $|(\omega-\omega^-)(t_s-t_0)| \ll 1$. Then we can make the small angle approximation in the sine and cosine function like we did before to show that the sine and cosine terms are small compared to the Si terms. If we just look at the first term:

$$\Delta(\omega)_1 = \frac{\alpha}{\pi^2\sigma^2}\int_{\omega^-}^{\omega^+}(\omega\prime-\omega_0)\frac{\sin[(\omega-\omega\prime)(t_s-t_0)]}{\omega-\omega\prime}d\omega\prime$$

$$= \frac{\alpha}{\pi^2\sigma^2}\Bigg[(\omega-\omega_0)[\mathrm{Si}((\omega-\omega^-)(t_s-t_0)) - \mathrm{Si}((\omega-\omega^+)(t_s-t_0)] + \frac{\cos[(\omega-\omega^-)(t_s-t_0)] - \cos[(\omega-\omega^+)(t_s-t_0)]}{(t_s-t_0)}\Bigg].$$

(44)

Then we can set $\cos[(\omega-\omega^+)(t_s-t_0)] \approx 1$ and $\cos[(\omega-\omega^-)(t_s-t_0)] \approx 1$ so that now:

$$\Delta(\omega)_1 = \frac{\alpha}{\pi^2\sigma^2}\int_{\omega^-}^{\omega^+}\omega\prime\frac{\sin[(\omega-\omega\prime)(t_s-t_0)]}{\omega-\omega\prime}d\omega\prime$$
$$= \frac{\alpha}{\pi^2\sigma^2}\Big[(\omega-\omega_0)[\mathrm{Si}((\omega-\omega^-)(t_s-t_0)) - \mathrm{Si}((\omega-\omega^+)(t_s-t_0)] + \frac{1-1}{(t_s-t_0)}\Big]$$
$$= \frac{\alpha}{\pi^2\sigma^2}\Big[(\omega-\omega_0)[\mathrm{Si}((\omega-\omega^-)(t_s-t_0)) - \mathrm{Si}((\omega-\omega^+)(t_s-t_0)]\Big]. \tag{45}$$

The first term of the expansion will be small compared to the Si terms, so we can eliminate the sine and cosine terms. We can then restore the Gaussian from its Taylor series:

$$\Delta(\omega) \approx \frac{1}{\sqrt{2\pi^3\sigma^2}}e^{-\frac{(\omega\prime-\omega_0)^2}{2\sigma^2}}\big[\mathrm{Si}((\omega-\omega^-)(t_s-t_0)) - \mathrm{Si}((\omega-\omega^+)(t_s-t_0))\big]$$
$$+\frac{\alpha}{\pi^2\sigma^2}\Big[\big((\omega-\omega_0) - \frac{(\omega-\omega_0)^3}{2\sigma^2} + \frac{(\omega-\omega_0)^5}{8\sigma^4} + ...\big)[\mathrm{Si}((\omega-\omega^-)(t_s-t_0)) - \mathrm{Si}((\omega-\omega^+)(t_s-t_0)]\Big]$$
$$= \frac{1}{\sqrt{2\pi^3\sigma^2}}e^{-\frac{(\omega-\omega_0)^2}{2\sigma^2}}\big[\mathrm{Si}((\omega-\omega^-)(t_s-t_0)) - \mathrm{Si}((\omega-\omega^+)(t_s-t_0))\big]$$
$$+\frac{\alpha}{\pi^2\sigma^2}\Big[(\omega-\omega_0)e^{-\frac{(\omega\prime-\omega_0)^2}{2\sigma^2}}[\mathrm{Si}((\omega-\omega^-)(t_s-t_0)) - \mathrm{Si}((\omega-\omega^+)(t_s-t_0)]\Big]$$
$$= \big(\frac{1}{\sqrt{2\pi^3\sigma^2}} + \frac{\alpha(\omega-\omega_0)}{\pi^2\sigma^2}\big)e^{-\frac{(\omega-\omega_0)^2}{2\sigma^2}}\big[\mathrm{Si}((\omega-\omega^-)(t_s-t_0)) - \mathrm{Si}((\omega-\omega^+)(t_s-t_0))\big]. \tag{46}$$

This is the form of the correction for small skewness $|\alpha| \ll 1$. Notice when $\alpha = 0$ then the equation for the correction of the Gaussian is restored. We can see that we get approximately our original frequency distribution times the Si terms back because of the following:

$$\Delta(\omega) \approx \frac{1}{\pi}\big(\frac{1}{\sqrt{2\pi\sigma^2}}(1 + \frac{\alpha(\omega-\omega_0)}{\sqrt{2}\sigma})e^{-\frac{(\omega-\omega_0)^2}{2\sigma^2}}\big)\big[\mathrm{Si}((\omega-\omega^-)(t_s-t_0)) - \mathrm{Si}((\omega-\omega^+)(t_s-t_0))\big]. \tag{47}$$

We recognize the first part of the equation as our original frequency distribution. If we have a frequency distribution $\tilde{S}(\omega)$ which is some Gaussian distribution with a small amount of skewness, then we can expect to get a correction of approximately proportional to the distribution. This matches the results of what we got for the case when $\tilde{S}(\omega)$ is a pure Gaussian:

$$\Delta(\omega) = \frac{1}{\pi}\int_{\omega^-}^{\omega^+}\tilde{S}(\omega\prime)\frac{\sin[(\omega-\omega\prime)(t_s-t_0)]}{\omega-\omega\prime}d\omega\prime \approx \frac{1}{\pi}\tilde{S}(\omega)\big[\mathrm{Si}((\omega-\omega^-)(t_s-t_0)) - \mathrm{Si}((\omega-\omega^+)(t_s-t_0))\big], \tag{48}$$

for $|(\omega-\omega^+)(t_s-t_0)| \ll 1$ and $|(\omega-\omega^-)(t_s-t_0)| \ll 1$ with skewness $|\alpha| \ll 1$. Like we said for the Gaussian frequency distribution if we make the frequency distribution into a step function with some bounds within the collimator aperture, then we recovered the exact result of the background for the step function frequency distribution. This means that even for a slightly skewed Gaussian distribution we can use the Si functions to approximate the background. since we know the step function and Gaussian backgrounds are almost the same, we can also know that a Gaussian frequency background can be used for a slightly skewed Gaussian for small start times.

The triangular fitting function will work better for a skew Gaussian because the triangular frequency distribution can be asymmetric so we do not have to make the assumption that $|\alpha| \ll 1$. This is why the step function, Gaussian, and triangle frequency distributions all yield equivalent fitting for an asymmetric frequency distribution up to about 20 $\mu$s after which the approximation breaks down and the triangle frequency distribution is superior since it relies does not rely on the assumption that $|\alpha| \ll 1$.

# C Approximating the step function to be a Dirac delta function

The background for a delta function frequency distribution is the same as the other frequency distributions for small values of $t_s$ shown in figure 7. In the last appendix B we showed that we could use the Gaussian and Step function backgrounds to either a Gaussian or skew-Gaussian frequency distribution when $t_s$ is small.

Here we will show that the step function and the delta function frequency distributions also has the same approximate form when $t_s$ is small. This is not surprising since the delta function is a step function with infinite hight and infinitely small width. We also showed that the step function, Gaussian, and triangle functions are all similar, so in the limit where the frequency distribution is approximately symmetric and $t_s$ is small, all of the fit functions used are approximately equivalent.

## C.1 Spherical Bessel function

We can approximate the Si function as a sum of spherical Bessel functions [11]:

$$\mathrm{Si}(2x) = 2x \sum_{n=0}^{\infty} [j_n(x)]^2, \tag{49}$$

where $j_n$ is the nth spherical Bessel function defined by the following:

$$j_n(x) = (-x)^n \left(\frac{1}{x}\frac{d}{dx}\right)^n \frac{\sin(x)}{x}. \tag{50}$$

The first three spherical Bessel functions of the first kind will be the following:

$$j_0 = \frac{\sin(x)}{x} \tag{51}$$

$$j_1 = \frac{\sin(x)}{x^2} - \frac{\cos(x)}{x} \tag{52}$$

$$j_2 = \left(\frac{3}{x^3} - 1\right)\frac{\sin(x)}{x} - \frac{3\cos(x)}{x^2}. \tag{53}$$

$$\tag{54}$$

With the assumption that our argument of the Si function $|(\omega - \omega^+)(t_s - t_0)| \ll 1$ and $|(\omega - \omega^-)(t_s - t_0)| \ll 1$ then we can approximate the summation to only include the first spherical Bessel function $j_0$ such that:

$$\mathrm{Si}(x) \approx x j_0(x/2)^2 = x\,\mathrm{sinc}(x/2)^2 = 2\sin(x/2)\,\mathrm{sinc}(x/2). \tag{55}$$

### C.2 sinc background approximation

We can plug in this the approximation in equation (55) into our approximate equation for the background with Gaussian frequency distribution (36):

$$\Delta(\omega) = \frac{1}{\pi}\int_{\omega^-}^{\omega^+} \tilde{S}(\omega\prime)\frac{\sin[(\omega-\omega\prime)(t_s-t_0)]}{\omega-\omega\prime}d\omega\prime \approx \frac{1}{\pi}\tilde{S}(\omega)\big[\,\mathrm{Si}((\omega-\omega^-)(t_s-t_0)) - \mathrm{Si}((\omega-\omega^+)(t_s-t_0))\big]$$
$$\approx \frac{-2}{\pi}\tilde{S}(\omega)\big[\sin[\frac{(\omega-\omega^+)(t_s-t_0)}{2}]\,\mathrm{sinc}[\frac{(\omega-\omega^+)(t_s-t_0)}{2}] - \sin[\frac{(\omega-\omega^+)(t_s-t_0)}{2}]\,\mathrm{sinc}[\frac{(\omega-\omega^-)(t_s-t_0)}{2}]\big]. \tag{56}$$

We can see that the correction term is proportional to a sinc but we can further simplify to:

$$\Delta(\omega) = \frac{1}{\pi}\int_{\omega^-}^{\omega^+} \tilde{S}(\omega\prime)\frac{\sin[(\omega-\omega\prime)(t_s-t_0)]}{\omega-\omega\prime}d\omega\prime \approx \frac{1}{\pi}\tilde{S}(\omega)\big[\,\mathrm{Si}((\omega-\omega^-)(t_s-t_0)) - \mathrm{Si}((\omega-\omega^+)(t_s-t_0))\big]$$
$$\approx -\frac{2}{\pi}\tilde{S}(\omega)\big[\sin[\frac{(\omega-\omega^+)(t_s-t_0)}{2}]\,\mathrm{sinc}[\frac{(\omega-\omega^+)(t_s-t_0)}{2}] - \sin[\frac{(\omega-\omega^-)(t_s-t_0)}{2}\,\mathrm{sinc}[\frac{(\omega-\omega^-)(t_s-t_0)}{2}]. \tag{57}$$

Then when we use the exact form of the background of the step function frequency distribution (22):

$$\Delta(\omega) \approx \frac{1}{\pi}\frac{\sin[(\omega-\frac{(\omega^+ + \omega^-)}{2}))(t_s-t_0)]}{(\omega-\frac{(\omega^+ + \omega^-)}{2})}. \tag{58}$$

We restrict the bounds from the collimator aperture $\omega^+$ and $\omega^-$, to two points inside it, denoted as $\omega_2$ and $\omega_1$, to get a generalized equation:

$$\Delta(\omega) \approx \frac{1}{\pi}\frac{\sin[(\omega-\frac{(\omega_2 + \omega_1)}{2}))(t_s-t_0)]}{(\omega-\frac{(\omega_2 + \omega_1)}{2})}. \tag{59}$$

If our distribution is symmetric about some frequency $\omega_0$ such that $\frac{(\omega_2+\omega_1)}{2} = \omega_0$ then we can rewrite the background to explicitly show it is a sinc function:

$$\Delta(\omega) \approx \frac{1}{\pi}\frac{\sin[(\omega-\omega_0)(t_s-t_0)]}{(\omega-\omega_0)}, \tag{60}$$

which holds so long as $|(\omega-\omega_0)(t_s-t_0)| \ll 1$. We can then conclude that for sufficiently small values of $t_s$, we can use the sinc function to fit the background, even when the frequency distribution is Gaussian or skew-Gaussian, since the Si functions are approximated to be the sinc function , and we showed in section B that the Si function can be fitted to Gaussian or skew-Gaussian frequency distributions.

For a highly asymmetric frequency distribution, we can fit the background of the cosine Fourier transformation with a sinc function for at least the first 10 $\mu$, and with Si and erfi function for at least 20 $\mu$s, but for greater values of $t_s$ the triangle frequency distribution is superior since it does not assume the frequency distribution is approximately symmetric.

## References


[1] A. Chapelain, J. Fagin, D. Rubin, D. Seleznev, *Cornell fast rotation Fourier method*, GM2-doc-18901

[2] A. Chapelain, D. Rubin, D. Seleznev, *Extraction of the Muon Beam Frequency Distribution via the Fourier Analysis of the Fast Rotation Signal*, E989 note 130, GM2-doc-9701

[3] A. Chapelain, J. Fagin, D. Rubin, D. Seleznev, *Cornell fast rotation Monte Carlo method and user guide*, GM2-doc-COMING-SOON

[4] See 'TMC #3' in: GM2-doc-13759

[5] Y. Orlov et al., NIM A 482 (2002) 767-755.

[6] A. Chapelain, J. Fagin, D. Rubin, D. Seleznev, *Extraction of the radial distribution of the stored muon beam for the Run–1 60–hour data set via the the Cornell fast rotation Fourier method: estimation of the electric field correction to the anomalous spin precession frequency*, GM2-doc-COMING-SOON

[7] A. Chapelain, J. Fagin, D. Rubin, D. Seleznev, *Extraction of the radial distribution of the stored muon beam for the Run–1 9–day data set via the the Cornell fast rotation Fourier method: estimation of the electric field correction to the anomalous spin precession frequency*, GM2-doc-COMING-SOON

[8] A. Chapelain, J. Fagin, D. Rubin, D. Seleznev, *Extraction of the radial distribution of the stored muon beam for the Run–1 end game data set via the the Cornell fast rotation Fourier method: estimation of the electric field correction to the anomalous spin precession frequency*, GM2-doc-COMING-SOON

[9] A. Chapelain, J. Fagin, D. Rubin, D. Seleznev, *Extraction of the radial distribution of the stored muon beam for the Run–1 high kick data set via the the Cornell fast rotation Fourier method: estimation of the electric field correction to the anomalous spin precession frequency*, GM2-doc-COMING-SOON

[10] A. Chapelain, J. Fagin, D. Rubin, D. Seleznev, *Performance study of the Cornell fast rotation Fourier analysis with toy Monte Carlo simulations*, GM2-doc-19132

[11] Harris, F. E. *Spherical Bessel Expansions of Sine, Cosine, and Exponential Integrals* Appl. Numer. Math. 34, 95-98, 2000.

[12] A. Chapelain, J. Fagin, D. Rubin, D. Seleznev, *Cornell fast rotation Fourier analysis user guide*, GM2-doc-COMING-SOON